1-1-2006

Laser welding of thin sheets of galvanized steel and aluminum alloy

Weichiat Chen
Iowa State University

Laser welding of thin sheets of galvanized steel and aluminum alloy

by

Weichiat Chen

A thesis submitted to the graduate faculty

in partial fulfillment of the requirements for the degree of

MASTER OF SCIENCE

Major: Mechanical Engineering

Program of Study Committee:
Palaniappa A. Molian, Major Professor
Abhijit Chandra
L. Scott Chumbley

Iowa State University
Ames, Iowa
2006

Graduate College
Iowa State University

This is to certify that the master's thesis of

Weichiat Chen

has met the thesis requirements of Iowa State University

Signatures have been redacted for privacy

TABLE OF CONTENTS

LIST OF FIGURES

LIST OF TABLES

ABSTRACT

The purpose of this research was to develop novel laser welding methods to improve the quality and performance of thin-sheet metal joints. Dual-beam laser welding of aluminum and laser welding of zinc-coated steel were performed. A pulsed Nd:YAG laser was used as the welding laser while an auxiliary continuous wave diode laser was used as a pre-heating source in lap welding of two 50-μm aluminum sheets. The weld quality was then examined under scanning electron microscope and evaluated using micro-indentation hardness tester. Results show that deeper weld penetrations and higher tensile strengths were obtained using the dual-beam laser welding technique when compared to that of single beam Nd:YAG laser welding.

Joining of zinc-coated steels has proved to be a challenging problem because of the vaporization of low boiling temperature zinc during the welding process resulting in a number of weld defects. A "Vent hole" approach, in which the 0.68 mm (24-gauge) galvanized steel sheets were pre-drilled using a pulsed Nd:YAG laser and then welded in lap-joint configuration using a 1.5 kW continuous wave CO_2 laser. With the addition of vent holes, zinc vapors were able to escape through the weld thus reducing weld defects such as porosity, spatter, and loss of penetration. The quality of the welds was inspected under optical and scanning electron microscopes and the properties were determined by tensile/hardness tests. Results are compared with those obtained in the conventional procedure of a constant joint gap between the sheets.

The study revealed that novel techniques further enhance the capabilities of lasers in thin-sheet metal welding useful for automotive, electronic and consumer industries.

CHAPTER 1. GENERAL INTRODUCTION

Introduction

Joining of thin metal sheets has many applications in today's world. Manufacturers in the Informational Technology and Networking, telecommunications, consumer electronics, and the automotive industry are striving to pack as many features into their products as possible. While this will increase the overall product weight and volume, manufacturers are finding ways to produce products that are ever smaller and denser without adding too much weight to the end products.

Conventional resistance welding that requires extensive electrode replacements and MIG/TIG welding that induces unacceptable heat-affected-zones are both unfit for joining small and delicate parts. Laser welding is very attractive for its numerous benefits such as minimum heat-affected-zone, ease of interface with robots, precision, and applicability to a variety of materials. The laser also finds its use in joining small, thin-walled objects such as hypodermic tubing, pacemaker cases, and diaphragms. The Carbon Dioxide (CO_2) and the Neodymium-doped Yttrium Aluminum Garnet (Nd:$Y_3Al_5O_{12}$ or Nd:YAG) lasers remain as the two most widely used sources for welding.

The purpose of this research is to investigate Computer laser welding of thin metal sheets by using CO_2 and Nd:YAG lasers in the aforementioned industries. Galvanized steel and aluminum alloy were chosen as the materials for this research because of their numerous applications and required intricacy in joining. Better welding techniques are deemed necessary in joining these materials. In this work, several welding approaches were attempted

and results were compared and analyzed to determine the best possible approach or method for obtaining high-quality welds.

Thesis Organization

This thesis consists of five chapters. Two of these Chapters are manuscripts submitted to journal or conference. Each manuscript will appear as a separate chapter as described in the Graduate College Thesis Manual. A brief introduction of the welding and objectives of the research are presented in Chapter 1. Literature review of recent developments in laser welding is provided in Chapter 2. Also included in this chapter are laser welding mechanism, types of laser welding, a comparison between laser welding and conventional welding, and problems encountered in laser welding of galvanized steel and aluminum alloys.

In Chapter 3, a paper titled "Dual-Beam Laser Micro Welding of 5052 Aluminum" describes the methods and analysis of lap welding of 50 μm thick 5052-H32 aluminum sheets without filler metals. In this paper, a pulsed Nd:YAG laser was used to weld the aluminum thin sheets, while an auxiliary continuous-wave diode laser was used as a pre-heating source. The integrity of the welds produced by employing the dual-beam laser welding technique was compared to those produced by single Nd:YAG laser welding. Chapter 4 presents the paper titled "CO_2 Laser Welding of Galvanized Steel Sheets Using Vent Hole Approach", a paper submitted to *Journals of Materials Processing Technology* is currently in the review process (manuscript number: NA-075). By implementing the novel "vent hole" approach, holes were pre-drilled on the galvanized steel sheets using a pulsed Nd:YAG laser. This allowed the zinc vapors to escape through the weld zone without causing expulsion of molten metal and associated defects such as porosity, spatter, and loss

of penetration. The quality of the welds was evaluated through optical and scanning electron microscopes and tensile/hardness tests. Results are then compared with those obtained in the conventional welding practice, which a constant joint gap is placed between the sheets. The conclusions drawn from this research are presented in Chapter 5.

CHAPTER 2. LITERATURE REVIEW

Introduction to Laser Welding

Initial studies were conducted on laser welding in the late 1960s mainly for the microelectronics industry; however the aerospace industry was the first to apply laser welding in mid 1970s after their prior experience with electron beam welding. Laser welding has all the benefits provided by the electron beam welding; in addition, a vacuum chamber and X-ray shielding are not needed for laser welding. At present, laser welding is a proven joining technique in automotive, metals (parts supply), shipyard, microelectronics, packaging and aerospace industry [1, 2]. With laser welding, vast selections of materials are able to be joined together with ease.

Today, laser welding often finds its uses in metalworking industry, routinely producing welds for common items such as cigarette lighters, watch springs, motor/transformer lamination, hermetic seals, battery and heart pacemaker and electronics [3, 4, 5]. Laser welding is used in place of many different standard processes, such as resistance (spot or seam), submerged arc, RF induction, high-frequency resistance, ultrasonic and electron-beam [4].

Laser Welding Mechanism

Laser welding represents a delicate balance between heating and cooling within a spatially localized volume overlapping two or more solids such that a molten pool is formed and remains stable until solidification is completed [6]. In laser welding, the incident laser beam is focused on a component above its melting point to create a melt pool which is then

grown and allowed to flow into the interface between the components that are to be joined. The molten material is solidified rapidly, forming a fusion bond that secures the components together with high strength. Because of the small heat input per unit volume, weld distortion is small. However, the weld integrity may be compromised by vaporization of alloy components, excessive thermal gradients that lead to cracking on solidification, and instabilities in the volume and geometry of the weld pool that results in porosity and void formation [6].

Laser welding is very sensitive to the focusing property of the laser beam. The laser intensity is at its highest at focus, and drops rapidly away from the focus point. In laser welding process, laser beam is brought to focus on or very near to the surface of the workpieces that are to be joined [7]. When the incident laser beam irradiates the highly reflective metal surface, a large percentage of the beam is reflected away. The remaining laser beam energy, absorbed quickly, heats up the workpiece and reduces the surface reflectivity. There are basically two types of welding mechanisms known as conduction welding and keyhole welding.

Conduction Welding

In conduction welding, laser energy is deposited onto the surface of the workpiece via the incident beam until the surface melts [8 – 10]. A hemispherical molten pool is created around the laser beam focal spot. Heat is then transported from the molten pool deeper into the workpiece by means of heat conduction (Figure 2.1 a). This is achievable by using a power density of lower than 10^6 W/cm^2 and is commonly seen with the use of low power

pulsed lasers like the Nd:YAG. Due to the low power density nature of conduction welding, the thicknesses of the materials to be joined are limited. In conduction welding, the laser beam spot size is comparable to the sheet thickness and laser intensity is only adequate to cause melting the metal without evaporation. In some alloys, high cooling rates that are associated with high welding speeds may result in weld embitterment or heat affected zone. Conduction welding, which uses a lower power density is comparatively stable and may offer an alternative mean of welding traditionally difficult materials such as aluminum alloys.

Keyhole Welding

Keyhole welding or sometimes referred to as deep penetration welding (Figure 2.1 b) is characterized by heating up the workpiece to a temperature above the boiling point of the workpiece material until the material starts to evaporate on the surface. At high power densities ($>10^6$ W/cm^2), the molten material with high vapor pressure overcomes its surface tension and moves out of the way of the beam [11]. A needle cavity full of ionized metallic and gas vapors is formed [12]. The nearly 100% absorptive cavity enables laser energy to penetrate deeply into the workpiece; this is referred to as keyhole formation [13].

The beam melts the front wall of the cavity and the molten metal flows to the rear wall and back into the cavity where it solidifies as the beam moves away in the direction of the weld seam [14]. Since laser energy penetrates deep into the target and efficiently couples to the cavity walls, the beam forms a narrow weld with a high aspect ratio [14].

The keyholing process gives rise to violent plasma generation which consists of metal vapor, ionized atoms, and free electrons. Plasma resides both outside and inside the keyhole,

known as *plasma plume* and *keyhole plasma* respectively; and the bright and often bluish flash that is frequently seen during laser welding is the plasma plume above the keyhole [15]. This bright plasma can block, reflect, or refocus the laser beam, resulting in insufficient penetration, burn-through, irregular weld shape, or contamination of beam delivery optics and considerably decrease the melting efficiency [16].

Other problems associated with the keyhole welding are instability, keyhole oscillation, and intermittent closure of the keyhole that often leads to porosity [12]. A study [17] conducted on CW CO_2 laser welding reveals that by using pure nitrogen as shielding gas, keyhole instability was greatly reduced and porosity formation was effectively suppressed.

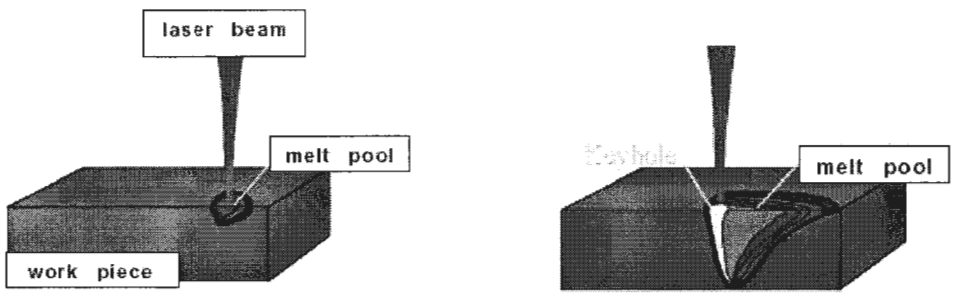

Figure 2.1. (a)conduction welding, (b) keyhole welding (source: Precitec Co.)

Comparison of Laser Welding and Conventional Welding

The laser keyhole welding technique transfers heat from the laser source into the material not to just a point on the surface, but to a line extending through the material thickness [18]. Laser welding provides many advantages over the conventional welding techniques; these advantages include:

- High welding speed. Laser welding with a beam power density of 10^6 W/mm^2 at the work surface permits welding speed of several meters per minute with a total heat input that is much lower than that or arc welding on a similar workpiece [18].
- High aspect ratio. Deep, narrow and near parallel weld shape is common with laser welding.
- Ease of interface with computer- controlled robots that provide high degree of accuracy, consistency, control, repeatability and flexibility [19].
- Ability to weld dissimilar materials and geometries [19, 20, 21].
- Allows several sheets of metals to be lap welded together in a single pass.
- Ability to reach into narrow gaps and access joint configurations that are often inaccessible by conventional welding techniques.
- Cost effective. Finishing step is often not necessary after laser welding [1].
- Very narrow heat affected zone (HAZ). The low heat input of laser welding results in narrow HAZ and little distortion compared to the convention welding.

Figure 2.2 a and b show keyhole laser welded stainless steel that is free of segregated eutectic and fused boundaries of grains in close vicinity to the HAZ; the structural transformations occurred is five or six times smaller than that in the arc weld and the size of grains in this region increases only slightly [14]. This structure not only improves its resistance to hot cracking, but also the mechanical properties of the weld. Figure 2e and Figure 2f reveal the difference between the microstructure of the laser-welded and TIG welded stainless steel 304. The laser weld exhibits smaller grain size than those observed in

the TIG weld.

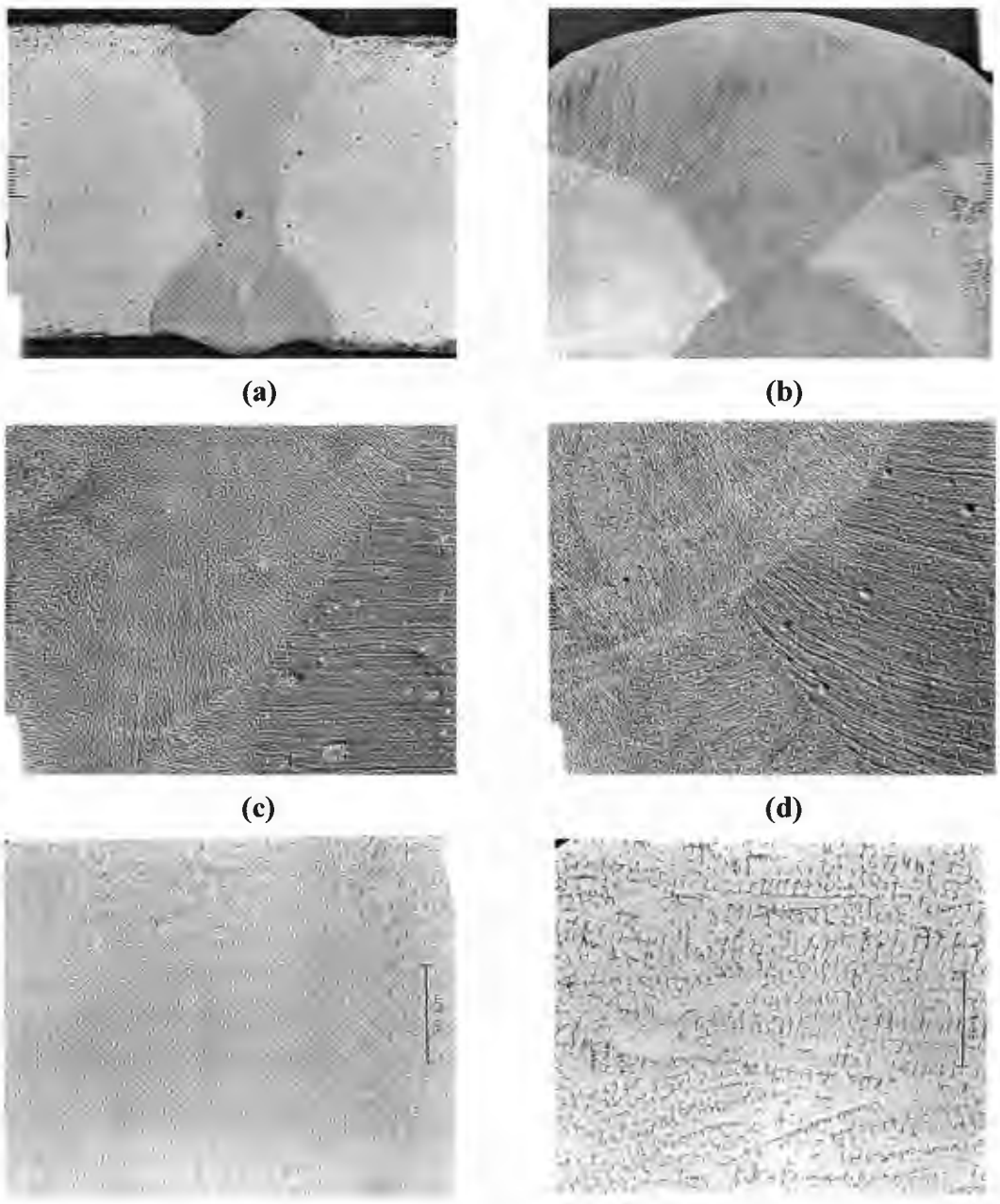

Figure 2.2. Butt welds produced by laser welding and TIG welding on 2mm SS304 sheets a,b) magnification: 25X; c,d) magnification:100X; e,f) magnification: 500X. (Source: P. Molian, Iowa State University Laser Lab)

CO_2 Laser Welding

The CO_2 laser, typically uses a gas mixture with 70 % He, 15 % CO_2 and 15 % N_2 [23]. He and N_2 in the mixture help remove unwanted wavelengths and promote photon generation efficiently. The properties of the mixture will vary from system to system. The overall efficiency is defined as the ratio of the useful power output to the total power input that reaches 10% for commercial CO_2 lasers. CO_2 lasers are available commercially with output powers ranging from 0.5 kW to 25 kW. CO_2 lasers are commonly larger, more complex and have output power much higher than the Nd:YAG lasers, which will be described later in this chapter. CO_2 lasers are powered by either a direct current (DC) or radio frequency (RF) high voltage system. Though highly efficient, this type of laser still requires input power that is ten times the laser output. Gas mixture within the laser is circulated through the resonator tubes and a heat exchanger cools down the gas temperature. A robust blower drives the lasing gas through the resonator tubes at high velocity. The gas is either flown co-axial with the optical axis (axial flow) or perpendicular to the optical axis (cross flow). An axial flow CO_2 laser sacrifices laser power for beam quality while a cross flow CO_2 laser gets higher output power for a given resonator length [18, 22]. A drawback of CO_2 lasers is that the light cannot be transmitted along fiber optic cables; therefore a system of mirrors is used. Because of the high reflectance of metals for the 10.6 μm wavelength light of CO_2 lasers, metallic mirrors are used to direct the beam [24]. Very precise coordination is necessary to direct the light to the correct location.

Nd:YAG Laser Welding

The Nd:YAG (Neodymium-doped Yttrium Aluminum Garnet) laser is a solid state pumped laser with an output wavelength of 1.06 μm, which is in the near IR. The active material in the YAG laser is triply ionized neodymium, Nd^{3+} and the host is a complex oxide with the chemical composition $Y_3Al_5O_{12}$. The optical cavity of the YAG laser consists of flash lamps, laser rod, reflector and mirrors. Current pulses generated by the power supply were sent to the flash lamps to produce white light. The white light would be then absorbed by the laser rod with the aid of the gold reflector assembly to excite the doped Nd atoms. These excited Nd atoms then produce light by spontaneous and stimulated emission, which results in generation of pulses laser light that is in sync with the current pulse from the power supply. Deionized water is fed to cool the laser rod, flash lamps and reflector to prevent thermal distortion that may otherwise degrade the laser efficiency [18, 22]. YAG lasers can be used for overlapping pulse seam welding and spot welding. Through frequency doubling and higher harmonic generation, YAG lasers are used for studies in material property, photochemical, and interactions in the visible and ultraviolet ranges. The light emitted by YAG lasers can be transmitted along flexible fiber optical cables. Because of this advantage, Nd:YAG lasers are finding increasing use in numerous applications.

However, the shortcomings of this type of laser is that the overall efficiency is limited to around 2–3 %, and the beam quality is inferior to that of a CO_2 laser [23]. Despite the shortcomings, many still prefer this technology because of its flexibility of being able to use fiber optics as the beam delivery system. Development of continuous wave, multi kilowatt Nd:YAG lasers, capable of fiber optical delivery, has within the past five years, extended the capabilities of these systems to produce welds in controlled environment previously

performed by the electron beam welding process [25].

At present, Nd:YAG laser welding is used commercially on a wide range of metals like C-Mn steels, coated steels, stainless steels, aluminum alloys, titanium and molybdenum. Applications of Nd:YAG laser welding can be seen in the electronics, packaging, domestic goods and automotive sectors. Significant interest has been shown more recently, particularly for the high power CW lasers, in the shipbuilding, oil and gas, aerospace and yellow goods sectors [26].

Laser Welding of Galvanized Steel

The automotive industry is seeking flexible and high quality welding methods for zinc-coated steels that are used in tailor blanks. A tailor-welded blank consists of steels of different gages, strengths and coating types welded together to produce a single blank prior to the forming process [27]. The application of tailor welded blanks dated back to the early 1980s when Thyssen used the technology in the production floors parts for the Audi 80 [28]. Since then the move towards increased use of Zn-rich coatings on steel sheets for automotive body applications has introduced many new difficulties, especially with welding of these materials. Laser welding without filler material is by far the most frequently used process for joining tailor blanks [29-31]. A CO_2 laser with a wavelength of 10.6 μm and power ranging from 1 to 10 kW is the most appropriate type [32].

Laser welding of zinc-coated steel has always been a challenge due to the low boiling point (906 °C) of zinc. The zinc coating evaporates violently at the weld interface resulting in high porosity joints upon solidifying. This problem is even more acute in lap joint

configuration. There are a number of approaches reported in the literature for fixing this problem, however, as of today; there is none that provides an easy and economical feasible solution [33].

Laser Welding of Aluminum Alloys

Aluminum alloys are strong, light, and corrosion resistant, which is why their applications are found in many branches of industries. Aluminum oxide tends to form as a thin film on the surface when aluminum alloys are heated to above their melting temperatures. This oxide has a high melting temperature (2273K) and absorbs water vapor and gases [14]. Measures have to be taken to prevent the oxides from contaminating the welds thus impairing the weld integrity.

Aluminum alloys that have higher thermal conductivity (ranging from 121 $W*m^{-1o}C^{-1}$ to 180 $W*m^{-1o}C^{-1}$) compared to that of carbon steels (36-54 $W*m^{-1o}C^{-1}$) [34] require a larger amount of energy for welding since aluminum alloys readily dissipate heat away during welding.

At temperatures below the aluminum alloy's melting temperature, a CO_2 laser with a 10.6 μm wavelength displays high reflectivity (0.97); combined with its high thermal conductivity and high heat capacity, a significant amount of laser energy is lost. At temperatures close to its melting point, the reflectivity falls sharply and allows deeper beam penetration. A further increase in beam power results in a linear increase in weld penetration.

References

1. Netherlands Institute for Metals Research. "Laser Welding." (Online) http://tmku209.ctw.utwente.nl/~nimrconsult/LaserIntro.htm, Jan. 2006.

2. Crafer, R. C. "Applications of lasers in manufacturing". Laser Welding, Cutting and Surface Treatment. Cambridge, England: The Welding Institute 1984.

3. Miller, Carl B. "US LASER CORP: Laser Welding Article." (Online) http://www.uslasercorp.com/envoy/welding.html, Jan. 2006.

4. Janssen, G. W. G. "Laser welding in the manufacture of heat pacemakers". Laser Welding, Cutting and Surface Treatment. Cambridge, England: The Welding Institute 1984.

5. Notenboom, G. J. A. M. "Laser spot welding in the electronics industry". ". Laser Welding, Cutting and Surface Treatment. Cambridge, England: The Welding Institute 1984.

6. Han, Wei. "Computational and experimental investigations of laser drilling and welding for microelectronic packaging". Ph.D. diss. Mechanical Engineering Department. Worcester Polytechnic Institute, Worcester, MA.

7. Dong, Yuanyuan. "Femtosecond pulsed laser ablation and patterning of 3C-SiC films on Si substrates for MEMS fabrication". Ph.D. diss. Department of Mechanical Engineering. Iowa State University, Ames, IA.

8. Okon, P, G. Dearden, K. Watkins, M. Sharp, P. French. "Laser Welding of Aluminium Alloy 5083." 21st International Congress on Applications of Lasers and Electro-Optics (ICALEO), Scottsdale, Oct 14-17, 2002

9. "Short description Laser Welding Monitor LWM" (Online) http://www.a-l-e.net/docs/infoLWM.pdf, Jan 2006.

10. "Laser Applications Newsletter" Laser Kinetics Inc. 11 Jan. 1998. Issue 1, vol 2 (Online) http://www.laserk.com/newsletters/lasernew2i1.html, Jan 2006.

11. Lee, Jae Y, Sung H. Ko, Dave F. Farson, Choong D. Yoo. "Mechanism of keyhole formation and stability in stationary laser welding." *J. Phys. D: Appl. Phys.* **35** (2002) 1570-1576

12. Belvito, Angelo. "Laser Material Processing: The Welding process." (Online) http://www.centrolaser.it/en/lavorazioni.html, Jan 2006.

13. Luxon, James T. and David E. Parker. Industrial Lasers and Their Applications Second Addition. New Jersey: Prentice Hall. 1992.

14. Grigoryants, Alexander G. Basics of Laser Material Processing. Moscow: CRC Press, Inc. 2000.

15. Tu, Jay F, Takashi Inoue and Isamu Miyamoto. "Qualitative characterization of keyhole absorption mechanisms in 20 kW-class CO_2 laser welding processes". J. Phys. D: Appl. Phys. **36** (2003) 192–203

16. Miyamoto, I and Maruo H 1992 Spatial and temporal characteristics of laser-induced plasma in CO2 laser welding *Proc. Laser Advanced Materials Processing LAMP'92* pp 311–16

17. Matsunawa, Akira and Seiji Katayama. "Keyhole Instability and Its Relation to Porosity Formation in High Power Laser Welding". Proceedings from Joining of Advanced and Specialty Materials, 5-8 Nov. 2001. Indianapolis, IN: ASM

International, 2002.

18. Dawes, Christopher. Laser Welding. Cambridge: Woodhead Publishing Ltd. 1992

19 "Lasers Offer Competitive Advantage Over Conventional Welding". LIA Today: Archives. (Online) http://www.laserinstitute.org/publications/lia_today/archive/articles/Lasers_Offer.htm ?article=articles/Lasers_Offer.htm, Jan 2006.

20. Kaul, Rakesh, P. Ganesh, and A. K. Nath. "Microstructural characterization of dissimilar laser weld between austenitic and ferritic stainless steels". *Journal of Laser Applications.* February 2005. Vol 17, Issue 1, pp. 21-29

21. Sun, Z. and J. C. Ion. "Review: Laser welding of dissimilar metal combination". Journal of materials science **30** (1995) 4205-4214.

22. Luxon, James T. and David E. Parker. Industrial Lasers and Their Applications Second Addition. New Jersey: Prentice Hall. 1992.

23. Legeleux, Fabrice. "Welding sees the light: Precision welding with lasers and robots." (Online) http://www.abb.com/global/abbzh/abbzh251.nsf!OpenDatabase&db=/global/gad/gad 02077.nsf&v=96DE&e=us&c=9056452CE30464BDC1256FBE0054A209, Jan 2006.

24. Appelt, D. and A. Cunha. "Beam delivery system for a CO_2 laser". *Laser Technologies in Industry (1988).* SPIE vol. 952 pp. 568-70.

25. Milewski, J. O., R. W. Carpenter, R. Nemec, A. Kelly, M. S. Piltch. "Refractory Metal Welding Using 3.3 kW Diode Pumped Nd:YAG Laser". Proceedings from

Joining of Advanced and Specialty Materials, 5-8 Nov. 2001. Indianapolis, IN: ASM International. 2002.

26. Hilton, Paul. "Nd:YAG laser welding." (Online) http://www.twi.co.uk/j32k/protected/band_3/kspah003.html, Jan. 2006.

27. Bratt, C. "Laser fabrication of tailored blanks". Ind. Laser User (11). May 1998. pp. 11-18

28. Waddell, W. and G. M. Davies. "Laser welded tailored blanks in the automotive industry". Weld. Met. Fabr. 63 (3) Mar. 1995. pp. 104-108

29. Riches, S. T. "Laser welding in automobile manufacture". Weld. Met. Fabr. 61 (1993) 79-83.

30. Ayres, K. R. and P. A. Hilton. "CO2 laser butt welding of coated steels for the automotive industry". Weld. Met. Fabr. 62 (1994) pp. 10-12.

31. Baron, J. S. "A cost comparison of weld technologies for tailored blanks". Welding Journal. 76 (1997) pp. 39-45.

32. Tušek, J., Z. Kampuš, and M. Suban. "Welding of tailored blanks of different materials". Journal of Materials Processing Techology 119 (2001) pp. 180-184.

33. Akhter, R., W. Steen, and D. Cruciani, Proceedings of 5th International Conference on *Lasers in Manufacturing, LIM 5,* 13-14, Sep.1988, Stuttgart, Germany, p.195

34. "Properties of Metals – thermal". (Online) http://www.engineersedge.com/properties_of_metals.htm, Jan 2006.

CHAPTER 3. DUAL-BEAM LASER MICRO-WELDING OF 5052 ALUMINUM

(A paper to be submitted to conference)

Weichiat Chen and Pal Molian

Abstract

Lap welding of 50 μm (0.002 in.) thick 5052-H32 aluminum sheets without filler metals using a dual-beam laser welding technique was investigated. A pulsed Nd:YAG laser was used to weld the aluminum thin sheets, while an auxiliary continuous-wave diode laser was used as a pre-heating source. The integrity of the welds was evaluated and compared to those produced by single beam Nd:YAG laser welding.

Introduction

The automobile and consumer electronics industries are striving to produce superior yet increasingly lighter, smaller, and stronger components. The miniaturizing trend and the introduction of micro-mechanical components in the industries make joining techniques more challenging. Laser was first introduced into the microelectronics industry in the late 60s for sealing electronic packages [1]. Since then laser welding becomes very attractive due to its numerous benefits, which include minimum heat-affected-zone, tight tolerance, ease of interface with robots, precision, and applicability to a variety of materials. The laser also finds its use in joining small, thin-walled objects such as hypodermic tubing, thin wire connections, pacemaker cases, and diaphragms. In contrast, conventional resistance welding

requires extensive electrode replacements and MIG/TIG welding induces unacceptable heat-affected-zones, making both unfit for joining fine and delicate parts.

The two lasers used for aluminum welding are CO_2 ($\lambda = 10.6$ μm) and Nd:YAG ($\lambda = 1.06$ μm). The benefits of CO_2 laser are lower operating costs, and better beam quality that results in uniform, consistent welds. However, the initial reflectivity of beam is very high, causing substantial energy loss. The reflectivity problem can be significantly minimized by using a shorter wavelength laser beam such as YAG. The absorptivity of Nd:YAG laser beam is about 3.16 times higher than that of CO_2 laser beam for metals [2]. Bagger et al reported that a 400 W pulsed Nd:YAG laser welds 30-40% deeper in stainless steel than a pulsed CO_2 laser of identical power [3]. Another beneficial aspect of YAG lasers is that the beam can be transmitted through fibers. YAG lasers appear to be more appropriate for welding delicate electrical components and small wires in medical equipment due to the fiber-optics beam delivery capability that in turn provides the flexibility in processing.

Aluminum alloys, well-known for their light weight, good formability and corrosion resistance, find many uses in sheet metal work, pressure vessels, aerospace and automotive applications. Recently, aluminum micro-welds are required in automotive electrical components and medical devices. A microweld is defined as the fusion zone having dimensions less than 100 μm [4].

Background

Aluminum poses three serious problems in laser welding: 1) the highly reflective nature of aluminum surface requires a high-intensity beam, and allows back reflection of the beam to the laser cavity damaging the optical components; 2) the high thermal

conductivity/diffusivity of aluminum reduces melt penetration; and 3) the high coefficient of thermal expansion induces deformation around the weld, leading to low-precision joints in micro-devices. For these reasons, it is extremely difficult to produce high-quality, stable aluminum welds. Thus, for successful micro-welding of aluminum, coupling of laser energy and careful optimization of laser parameters are deemed necessary.

Aluminum alloys are generally strain-hardened through cold work or heat treated by precipitation hardening. Cold-worked alloys undergo softening due to the heat introduced in laser welding. Heat treatable aluminum alloys (2000, 6000 and 7000 series) are susceptible to hot cracking during solidification and annealing of HAZ. There are two types of YAG lasers for aluminum welding: continuous wave (CW) and pulsed. CW lasers require much higher power than pulsed type. For example, 2-mm thick sheets of 5083 aluminum are welded using a 1.6 kW CW YAG in the bead-on-plate configuration at a welding speed of 0.5-m/min [5]. Requiring such high-power, CW YAG laser systems are complex, difficult-to-maintain, and costly. Pulsed lasers can reduce the average power to attain the required penetration but the occurrence of hot cracking during the rapid solidification and porosity due to loss of alloying elements are serious problems. Studies on aluminum alloy welds showed that an increase in the level of porosity was found to diminish the tensile strength [6, 7]. A 4% porosity level in weld volume reduces the weld tensile ductility by as much as 50% [7]. Filler metal may be used to circumvent such problems. The commonly observed weld defects in aluminum are solidification cracking (hot cracking), porosity, depletion of Mg and Zn, and loss of penetration. Solidification cracks were observed at the grain boundaries of columnar and equiaxed dendrites in almost all aluminum alloys that are welded with YAG lasers. Such cracks are preventable if the metal is preheated to 500° C.

Laser welding of aluminum alloys of the 5000, 6000, and 7000 series is accompanied by a loss of volatile elements such as Mg and Zn from the weld region. This has a profound negative effect on the composition and the properties of aluminum. The vaporization temperatures, shown in Figure 3.1, suggest that Mg, Zn, Cr, and Mn are susceptible to depletion during welding [8]. In one of the investigations, it was found that the Mg-content of evaporated particles is 20 times larger than the base alloy [9]. Porosity was mainly attributed to three sources: loss of alloying element through vaporization, entrapment of shield gas such as N_2, and dissolved H_2 in base alloys, and contamination. Vaporization of Mg in pulsed YAG laser welding seems to be the major contributor of porosity. Many alloys resist N_2 porosity. However, some alloys such as 5052 and 5083 trap extensively N_2. Filler metal addition and suitable shielding of the weld zone are the proper means to control the porosity. The loss of penetration is due to the initial reflectivity and large thermal conductivity of aluminum. However, evaporation of Mg assists in obtaining deeper penetration. The other problems include humping and undercutting (due to high speed) and spatter (due to high power, oxidation).

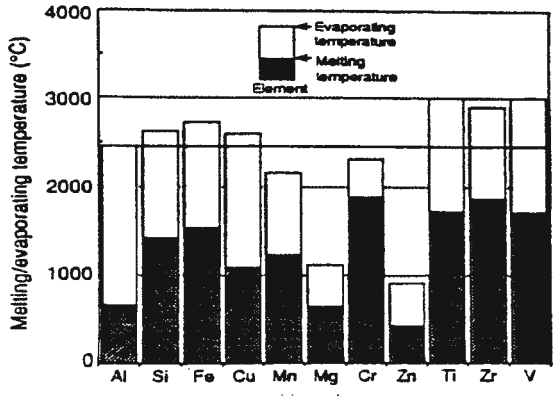

Figure 3.1. Melting and boiling points of elements (Source: Sakamoto et al. [8])

Some approaches to eliminate the defects associated with laser welding are:

1) Optimization of the waveform of laser pulse

Superpulsing or enhanced pulsing is usually employed particularly in spot welding to overcome the reflectivity problem and improve the penetration. Superpulsing involves a high-power spike pulse on the leading edge. However, this technique could not satisfactorily reduce the solidification cracking.

2) Use of high pulse energy, high repetition rate Nd:YAG lasers

Microscopic cracks are generally observed in YAG welding of aluminum, and this is attributed to the rapid solidification caused by low repetition rate. A high pulse energy, high repetition rate laser was reported [5] to produce crack-free welds especially in welding of 1-mm to 2-mm thick 5182 aluminum (5 Mg, 0.4 Cr, 0.25 Zn, 0.15 Cu, 0.35 Fe). Typical process parameters include 1 kW average power, 6 kW peak power, 60 J pulse energy, and > 10 Hz pulse repetition rate. Another interesting observation was that the variation in focal position up to 2-mm did not affect penetrations. The large tolerance allowed by this laser provided the flexibility of adding industrial robots for processing. However, this method did not generate crack-free overlap welds of 5052 alloy (2.5 Mg, 0.25 Cr) by any combination of parameters.

3) Dual-beam hybrid technique involving pulsed and CW YAG lasers

In this approach, a CW laser (500 W) was coupled with a pulsed laser (average power 700 W) to perform welding of 1-mm thick aluminum alloys. Experiments showed that for a laser power of 450 W and an auxiliary source power of 180 W, welding penetration obtained

was equivalent to that of a 1 kW laser [10]. Three different configurations were attempted. First, the CW laser beam was preceded by pulsed laser beam with a spacing of 1 mm, generating pre-heating effects. Second, both beams were impinged on the same spot, increasing the heat input. Third, pulsed laser beam was followed by CW laser beam, giving rise to post-heating effects [5]. Crack-free welds were obtained in all cases. However, the most optimum was found to be the pre-heating laser arrangement where the weld width was small.

In this paper, we extend the dual-beam concept by combining a CW diode laser and a pulsed Nd:YAG laser to produce high-quality welds in micro-welding of aluminum.

Experimental Details

The material used was A5052 alloy in the cold-worked condition, the composition of which is shown in Table 1. Typical additional impurities for 5000 series aluminum alloys were mainly Si, Fe, Cu, Cr and Ti [11]. The sheets of thickness 50 μm were procured and cleaned with acetone to remove grease and other surface contaminants. Theoretical values of reflectivity were estimated using the Drude theory. Beam reflection depends on the temperature of the metal, and is about 80% for temperatures near the melting temperature [10]. Although the reflectivity of aluminum was high (on the order of 90%), it decreases with an increase of temperature [2]. For this reason, diode laser was used to preheat the aluminum specimens prior to welding. The efficiency of a diode laser is 4-30 times greater than that of arc lamp- pumped Nd:YAG laser [12]. Diode laser emits light at a wavelength of 800 nm, which is considerably shorter than the most commonly used CO_2 and Nd:YAG lasers; this shorter wavelength enables a higher absorptivity in aluminum.

Single-Beam Laser Welding Experiment Setup

The sheets were secured on the welding platform using a special clamping device. A camera was placed directly above the welding platform and its line of sight was made coaxial to the Nd:YAG laser head by means of optics for monitoring the welding processes. The magnification of the camera lens was set at 50X for micro-welding purpose. A Lee Laser Model 712ST pulsed Nd:YAG laser operating in near TEM_{00} mode was used to weld the aluminum sheets in lap-joint configuration. A jack was then mounted underneath the welding platform. The aluminum sheets were brought to the laser beam focal point by adjusting the jack and monitoring the camera monitor. Throughout the experiments, the clamping device, welding platform and the jack were mounted on a linear motion table that is numerically controlled by a computer. Argon shielding gas was provided at a flow rate of 30 l/min to prevent excessive N_2 entrapment in the weld and the effects of moisture and contamination that otherwise cause porosity and cracking [13, 14]. The welding process was carried out using the pulsed Nd:YAG laser and shielding gas with welding speeds from 0.3 m/min – 0.9 m/min (0.2 $in.s^{-1}$ – 0.6 $in.s^{-1}$), average laser power ranging from 1.1 W – 3.6 W, and pulse repetition rates of 2 kHz to 20 kHz.

Dual-Beam Hybrid Laser Welding Experiment Setup

A second set of experiments using an additional CW diode laser emitting at a wavelength of 810 nm as an auxiliary source was conducted. The short wavelength laser beam was delivered via fiber optics into the welding chamber. The laser head was being secured on a fixture, inclined at an angle of 30° to the YAG welding laser. This pre-heating laser arrangement and the experiment set up are shown in Figure 3.2 and Figure 3.3

respectively. The temperature of incident diode laser beam was measured using a type-K thermocouple. The power of the CW diode laser was fixed at 5 W that gave a peak temperature of 732°C at the focal point. To prevent the lost of alloying elements such as Mg and Zn in 5052 alloy, the irradiance temperature of the pre-heating laser should be kept below 1100°C (see Figure 3.1). The dual-beam micro-welding process was conducted with the same welding parameters as previously with the single-beam laser welding process (see Table 3.2).

Table 3.1. Composition of 5052 aluminum alloy

Si	Fe	Cu	Mn	Mg	Cr	Zn	others	Al
0.25	0.4	0.1	0.1	2.2-2.8	0.15-0.35	0.1	0.15	balance

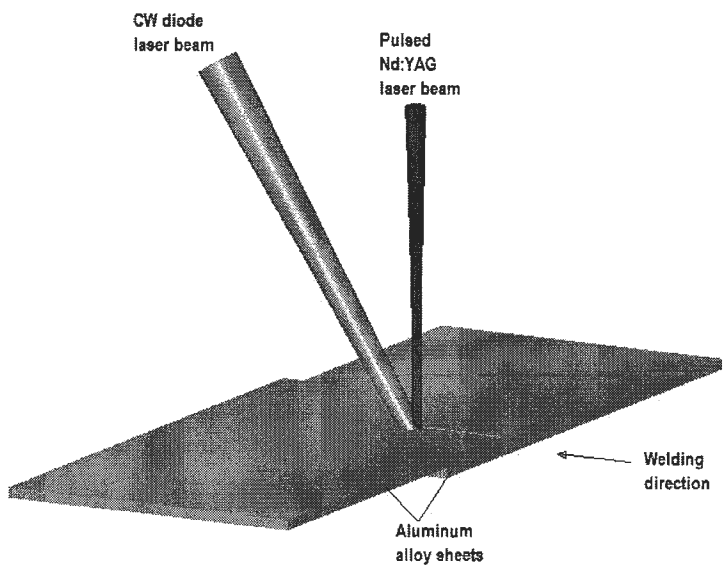

Figure 3.2. 3-dimensional schematic illustration of dual-beam laser micro welding of 5052 aluminum alloy sheets.

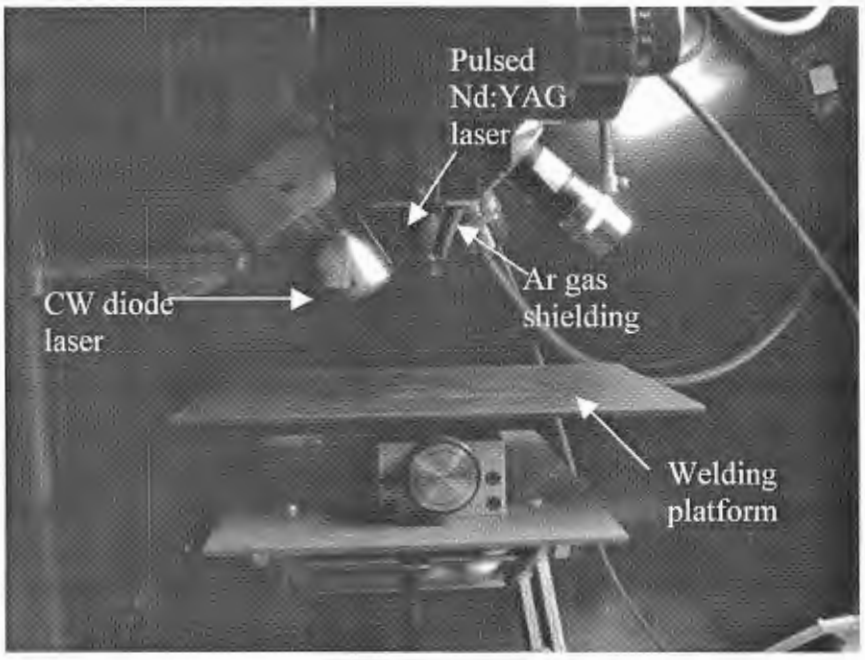

Figure 3.3. Experiment setup for Nd:YAG laser welding of aluminum sheets with CW diode laser as an auxiliary pre-heating source.

Table 3.2. Welding parameters for experiments.

Nd:YAG average laser power	1.1, 1.4, 2.0, 2.9, 3.6 W
Nd:YAG laser wavelength	1.064 μm
Welding Speed	0.3, 0.6, 0.9 m/min
Pulse repetition rate	2, 5, 10, 20 kHz
Pulse energy	0.55, 0.70, 1.00, 1.45, 1.80 mJ for 2 kHz
	0.22, 0.28, 0.40, 0.58, 0.72 mJ for 5 kHz
	0.11, 0.14, 0.20, 0.29, 0.36 mJ for 10 kHz
	0.06, 0.07, 0.10, 0.15, 0.18 mJ for 20 kHz
Diode laser power	5 W
Diode laser wavelength	800 nm

Welding process maps for both single-beam and dual-beam laser welding for three different welding speeds are shown in Figure 3.4a-f. It may be noted that the process parameter window for acceptable welding is slightly smaller for dual-beam laser welding processes particularly at lower welding speeds. Underfilling was discovered on the top of the weld seam when high average power and low pulse repetition rate (high pulse energy) were employed. The high pulse energy caused expulsion of the molten metal and also splatters on the surface. The addition of a pre-heating laser beam adds to the degree of underfilling, results in cutting instead of welding the sheets in some cases. At higher welding speed (0.9 m/min), the pre-heating beam assisted in reducing pulse energy and increasing repetition rate (Figure 3.4e, f).

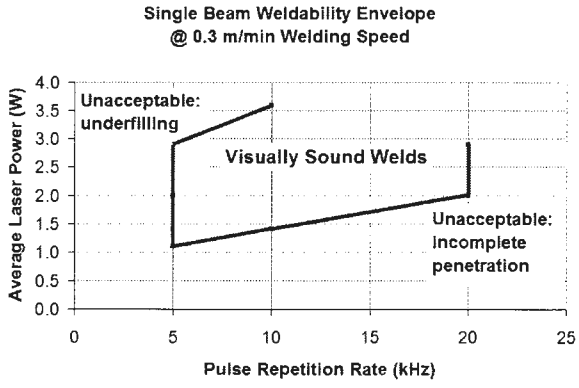

(a)

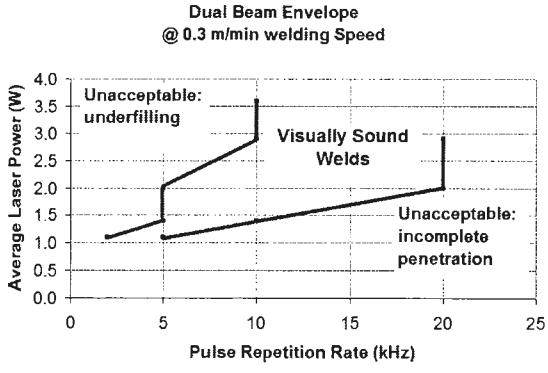

(b)

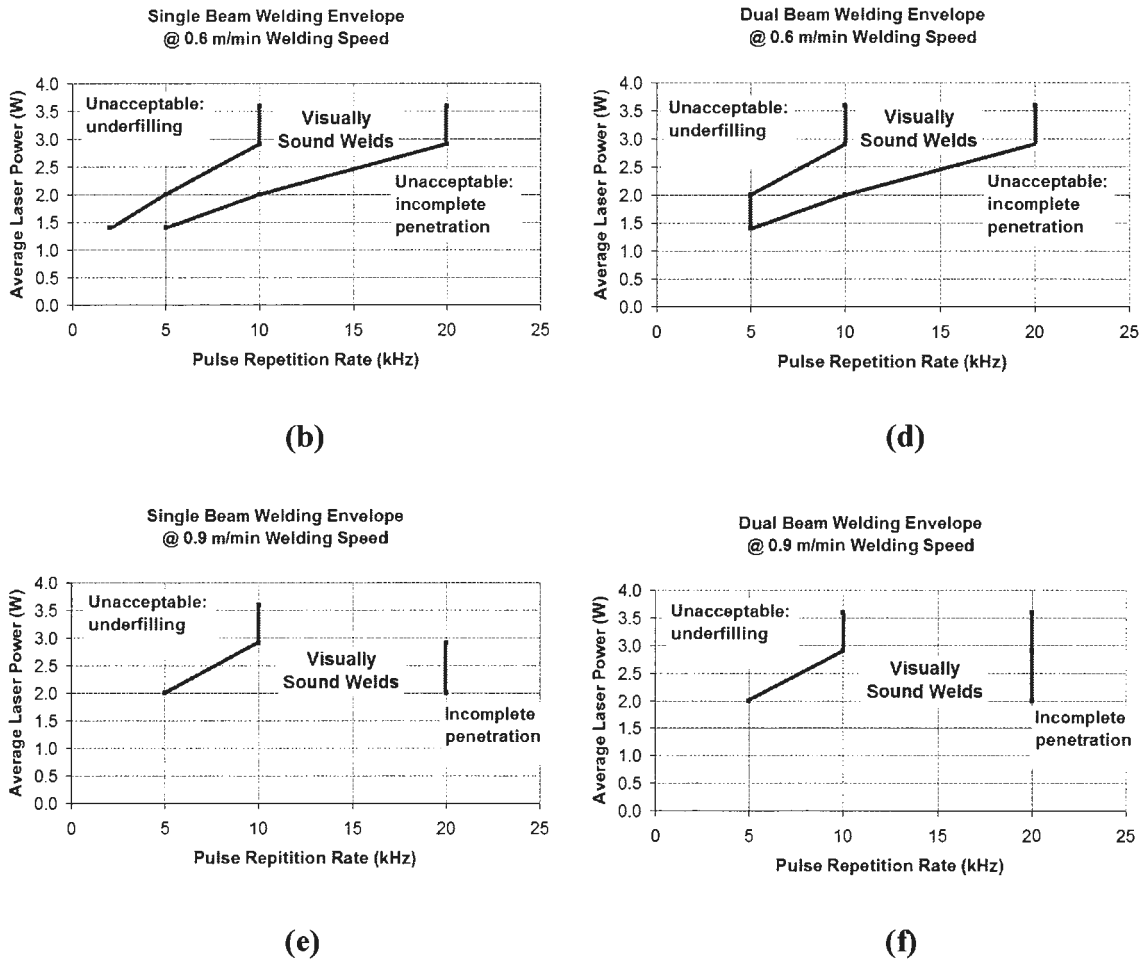

Figure 3.4. Welding envelopes at various welding speeds, average laser power and pulse repetition rates by using (a, c, e) single-beam laser welding; (b, d, f) dual-beam laser welding.

The integrity of the welds was evaluated using scanning electron microscope, and Vickers micro hardness indentation test. The simple micro-indentation test provides indirectly the tensile strength; typical tensile test testing of thin sheets proves ineffective [15]. The procedure for micro-indentation hardness is as follow: Vickers diamond pyramid indenter with a face angle of 136^{o} was used to indent the weld zone. A 200gf load was

applied on each of the weld seam through out the hardness test. A digital camera was attached to the eye piece of the hardness tester, and indentation images were sent to computer. By using ConfiDent software specially developed for measuring hardness, both diagonals of the indentation are easily measured and hardness numbers in Rockwell B-scale (HRB) and Vickers (HV) were obtained. Several indentations were made along the weld seam of and an average hardness number was recorded.

Results and Discussion

Figure 3.5a shows an optical micrograph of a representative transverse section of weld produced by single-beam Nd:YAG laser welding. A significant portion of the incident laser beam power was reflected off the surface causing the loss of coupling energy to the metal. The heat conducted from the top sheet to the bottom sheet was insufficient to melt the bottom sheet, resulting incomplete penetration. Figure 3.5b shows the weld produced by adding a pre-heating CW diode laser beam. More energy was coupled into the metal, which in turn deepened the weld penetration.

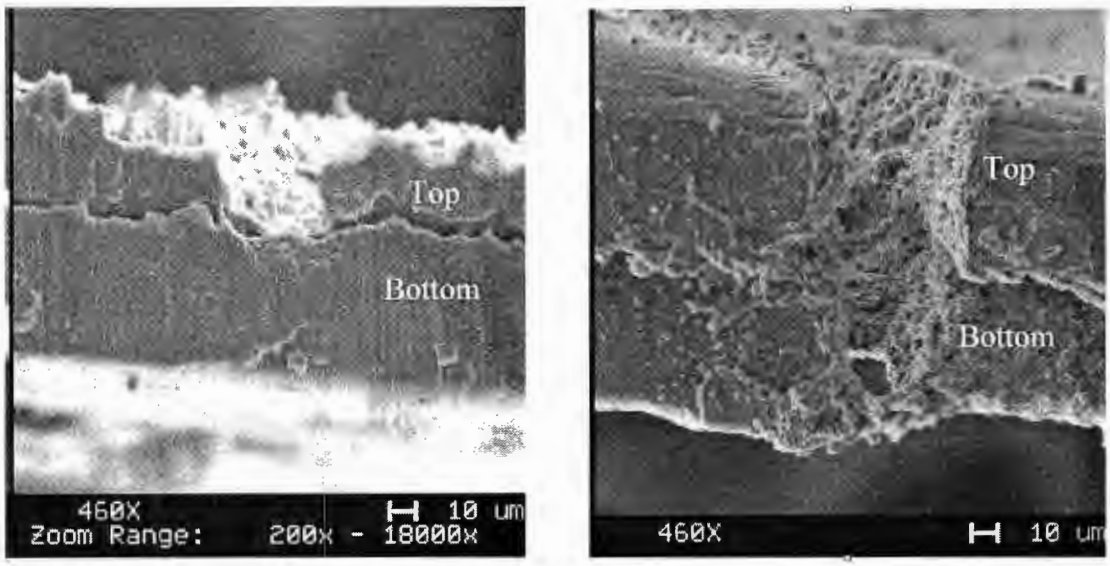

(a) (b)

Figure 3.5. Transverse section of Nd:YAG welds produced by micro-welding with 3.6 W average laser power, 0.9 m/min welding speed, and 1.8 mJ pulse energy: (a) single-beam welding resulted an incomplete penetration, (b) dual-beam laser welding produced much better penetration.

Figure 3.6a depicts an indentation made on the weld seam of a single-beam laser welded specimen. The weld has a mean hardness of 146 HV. Figure 3.6b indicates a smaller indentation on the weld seam produced by dual-beam laser welding, providing a higher hardness number of 182 HV (mean value). A similar micro-indentation hardness test was carried out on the weld seams of aluminum specimens with different welding parameters (Figure 3.7). It is confirmed that the hardness of welds produced by dual-beam laser welding process was higher than those welded by a single-beam laser.

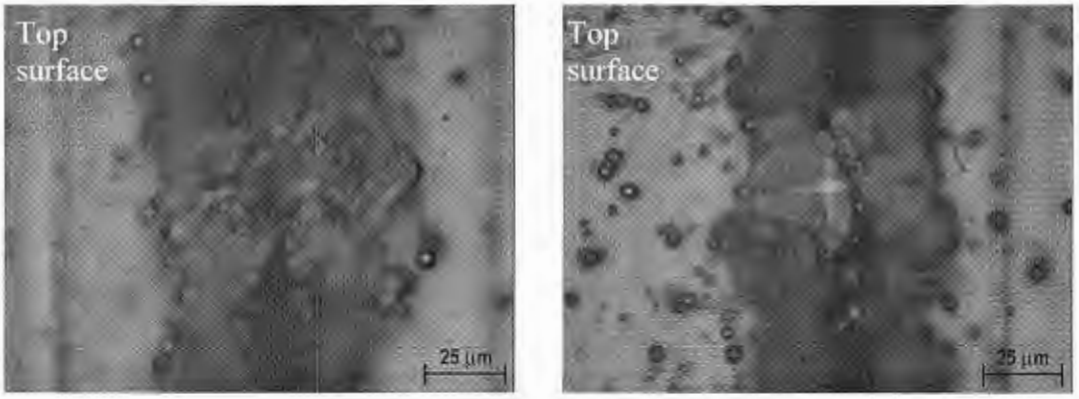

(a) (b)

Figure 3.6. Micrographs showing indentations from the hardness test of welds produced using average laser power of 3.6 W, pulse energy of 0.18 mJ, and a welding speed of 0.9 m/min with (a) single-beam laser welding, and (b) dual-beam laser welding.

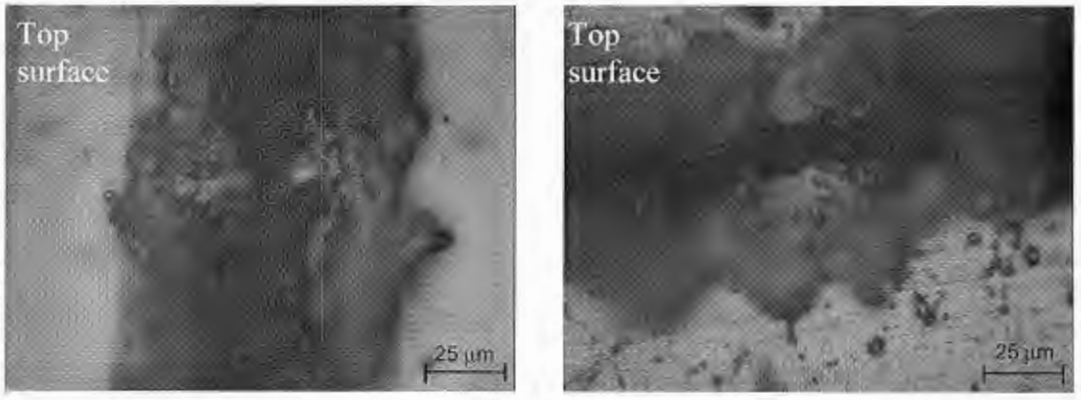

(a) (b)

Figure 3.7. Micrographs showing indentations from the hardness test of welds produced using average laser power of 1.4 W, pulse energy of 0.28 mJ, and a welding speed of 0.6 m/min (a) single-beam welding for a hardness of 84 HV, (b) dual-beam welding for an average hardness of 205 HV.

A histogram chart (Figure 3.8) gives a comparison of average hardness of welds produced by single-beam and dual-beam laser welding. At welding speeds of 0.3 m/min to 0.9 m/min, pulse energy of 0.18 mJ and an average laser power of 3.6 W, dual-beam laser welding provides welds with greater average hardness values.

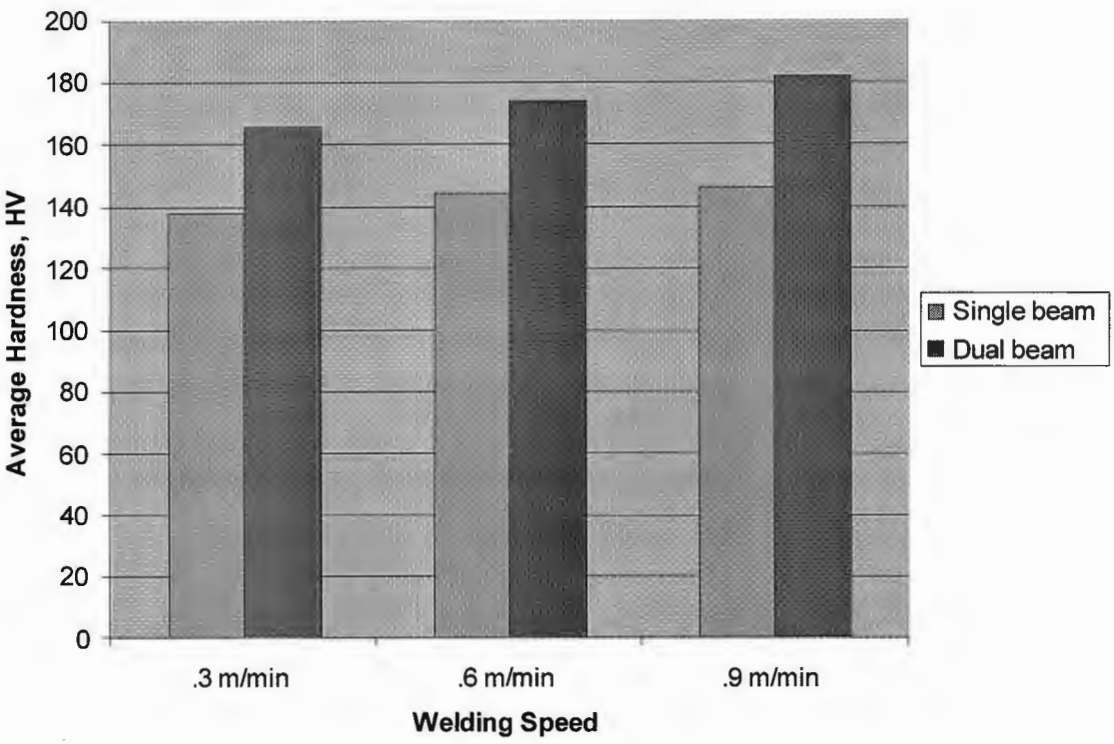

Figure 3.8. A comparison of mechanical properties of welds produced by single and dual beams.

Mathematical Model

A simple mathematical model based on heat conduction models (Carslaw et al) was used to compute the surface temperature rise caused by the pre-heating CW diode laser prior to welding [16]. The following assumptions were applied: 1) heat energy is uniform, 2)

semi-infinite slab of material, 3) laser radiation penetration is small relative to the laser beam diameter, 4) heat loss due to convection and radiation is negligible [17]. When the diode laser beam impinges the aluminum surface, the temperature can be calculated as

$$T(z,t)=\frac{2I}{K}\sqrt{kt}*ierfc\left(\frac{z}{2\sqrt{kt}}\right) \tag{3.1}$$

Where $T(z,t)$ is the temperature at depth z, and time t. K is the thermal conductivity, k is the thermal diffusivity, and I is the average power density absorbed into aluminum.

$$I = I_o(1-R)$$

I_o = incident power density and R = reflectance

$ierfc(x)$ is the integral of the complementary error function $erfc(x)$.

$$erfc(x)=1-erf(x)$$

$$erf(x)=\sqrt{\frac{2}{\pi}}\int_0^x e^{-x^2}dx$$

$$ierfc(x)=\frac{1}{\sqrt{\pi}}e^{-x^2}-x\cdot erfc(x)$$

The surface temperature at time t can be obtained from Eq. 3.1 by setting $z = 0$

$$T(0,t)=\frac{2I}{K}\sqrt{kt}*ierfc(0) \tag{3.2}$$

Since $ierfc(0)=\sqrt{\frac{1}{\pi}}$,

$$T(0,t)=\frac{2I}{K}\sqrt{\frac{kt}{\pi}} \tag{3.3}$$

Initially the aluminum workpiece is at room temperature. Heat supplied at $z = 0$ at the constant rate of I per unit time per unit area for time t_p. At time t_p the supply of heat ceases and the end $z = 0$ is thermally insulated. This condition matches the condition when the laser beam left the pre-heating spot (i.e. cool down). The temperature at a depth z and time t, is given by:

$$T(z,t) = \frac{2I}{K}\sqrt{k}\left[\sqrt{t} * ierfc\left(\frac{z}{2\sqrt{kt}}\right) - \sqrt{t-t_p} * ierfc\left(\frac{z}{2\sqrt{k(t-t_p)}}\right)\right] \qquad (3.4)$$

Where t_p is the time when supply of heat ceases (i.e the irradiance beam left the preheated zone).

Surface temperature of the workpiece when heat source has been turned off:

$$T(0,t) = \frac{2I}{K}\sqrt{\frac{k}{\pi}}\left[\sqrt{t} - \sqrt{t-t_p}\right] \qquad (3.5)$$

Using equation (3.3) and equation (3.5), surface temperature profile can be plotted as depicted in Figure 3.9. From the plot, surface temperature peaked at 424 °C and cooled down rapidly due to the high thermal diffusivity of aluminum. Since a-millimeter spacing was place between the pre-heating diode laser beam and the welding laser, it took 0.20 second for 0.3 m/min welding speed for the pre-heated spot to reach the welding beam. Refer to Appendix for thermal properties of aluminum alloy and sample calculations. Figure 3.9a reveals that the surface temperature was at 114 °C when the Nd:YAG laser welded the sheets resulting a temperature peak of 1385°C. The distance between the beams could be narrowed to reduce surface temperature drop thus increasing power coupled for welding.

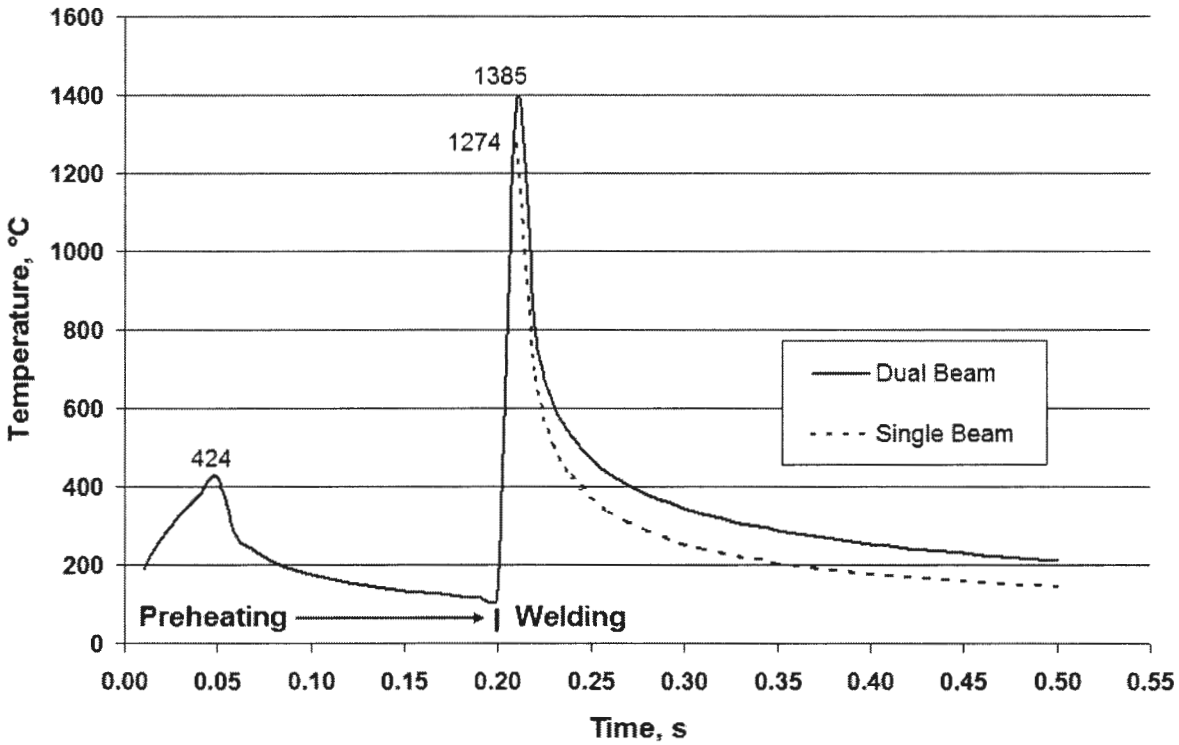
1600
1400
1200
1000
800
600
400
200
0
Temperature, °C
1385
1274
424
Dual Beam
Single Beam
Preheating
Welding
0.00
0.05
0.10
0.15
0.20
0.25
0.30
0.35
0.40
0.45
0.50
0.55
Time, s

(a)

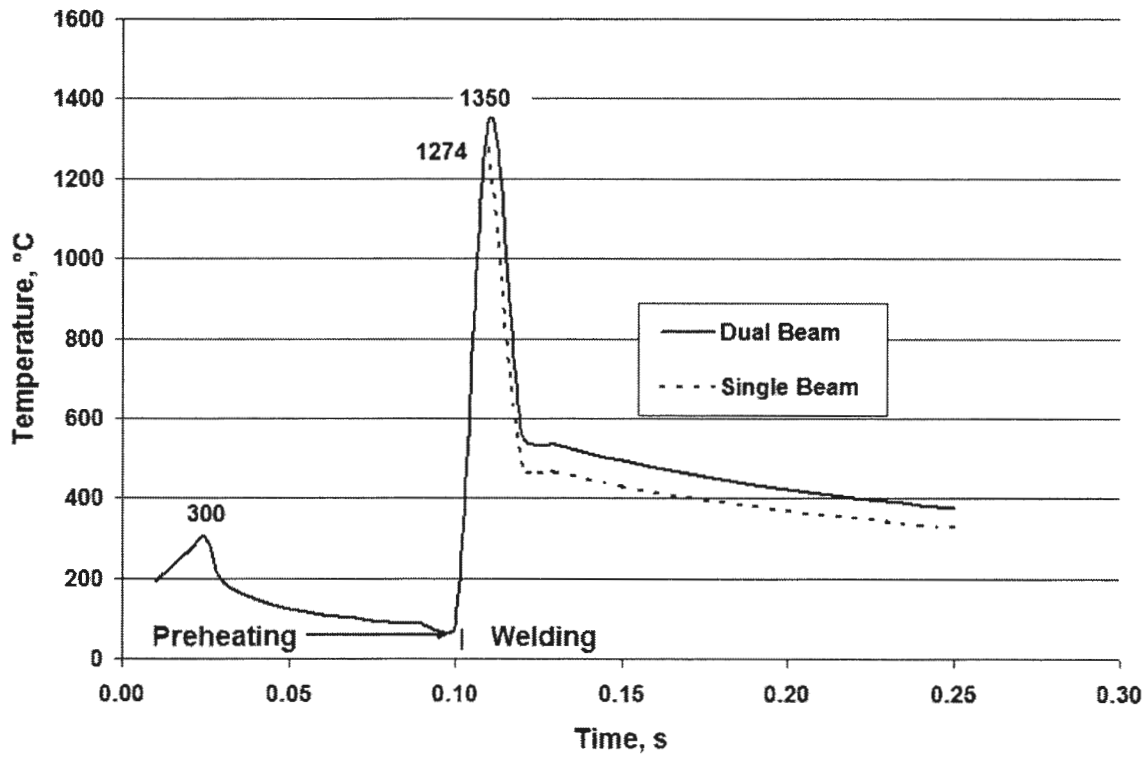
1600
1400
1200
1000
800
600
400
200
0
Temperature, °C
1350
1274
300
Dual Beam
Single Beam
Preheating
Welding
0.00
0.05
0.10
0.15
0.20
0.25
0.30
Time, s

(b)

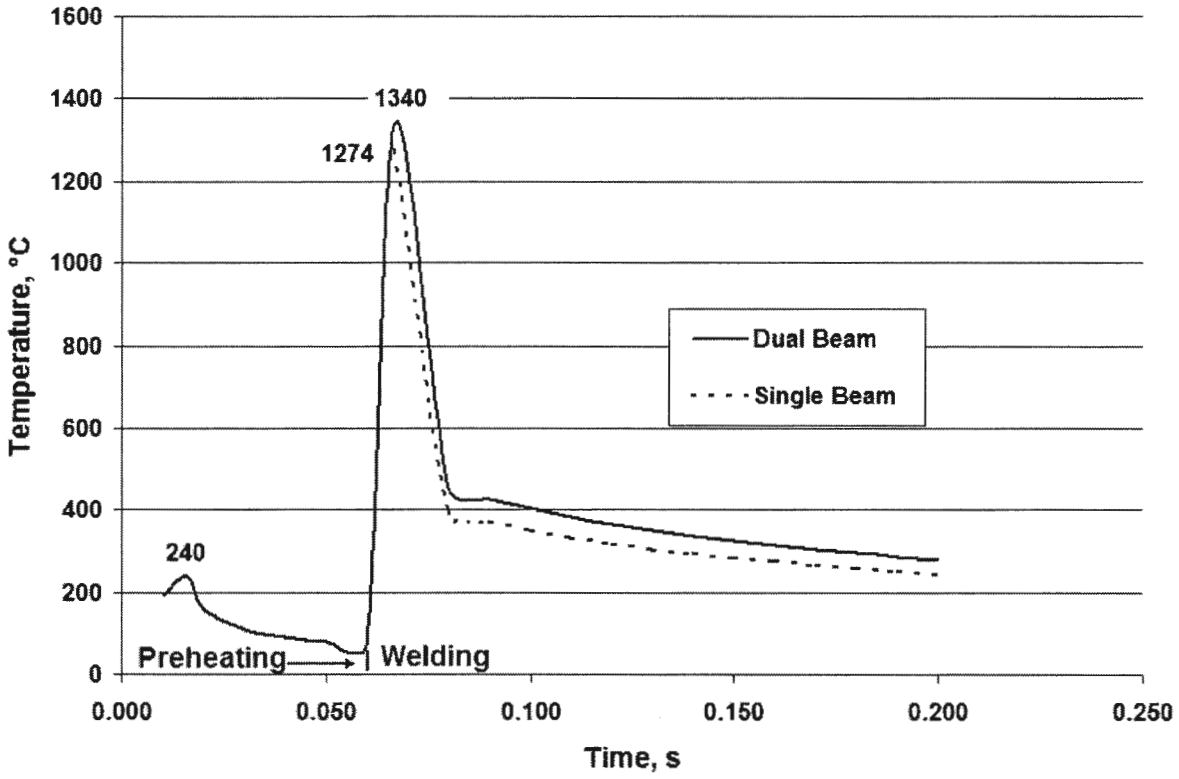

(c)

Figure 3.9. Dual-beam welding surface temperature profile with 5 W CW Diode laser preheating and 2 W pulsed Nd:YAG average power. (a) Welding speed = 0.3 m/min, (b) Welding speed = 0.6 m/min, (c) Welding speed = 0.9 m/min.

Conclusion

By using a short wavelength diode laser, more laser energy was able to be transferred to the aluminum that in turn enhanced the weldability of thin aluminum sheets in lap configuration. In addition, these diode lasers can be transmitted through fibers, improving the flexibility of the entire welding process.

In this work, laser welding of aluminum 5052 thin sheets with pulsed Nd:YAG laser and a CW diode laser as pre-heating source produced weld quality superior to that of welding

with a single pulsed Nd:YAG laser. Deeper weld penetrations and higher hardness (finer grain structures) were obtained using the dual-beam hybrid laser welding technique.

Acknowledgement

The authors would like to thank Professor Scott Chumbley (Ames Laboratory), Mr. Hal Sailsbury (Ames Laboratory), and Mr. Rajeev Madhavannair (Iowa State University), for providing their help and expertise in microscopy and NDE testing.

References

1. Rourke, M. Laser Based Manufacturing, CO_2 Systems. *Proceedings of the 1st International Conference on LASERS in manufacturing, 1-3 Nov. 1983*. Brighton, UK, pp. 231-241.
2. Xie, J. and Kar, A. Laser Welding of Thin Sheet Steel with Surface Oxidation. *Welding Journal*. October 1999, vol. 78, no. 10, pp. 343-348s.
3. Bagger, C., Laursen, S., Olsen, F. Comparisonn of a Pulsed CO2 laser and a Pulsed Nd:YAG Laser for Welding. *Proceedings of ICALEO '92 Laser Materials Processing, 25-29 Oct. 1992*. Orlando, Florida, pp. 537-546.
4. Semak, V. V., Knorovsky, G. A. and MacCallum, D. O. On the possibility of microwelding with laser beams. *Journal of Physics D: Applied Physics*. 2003. vol. 36, pp. 2170-2174.
5. Aruga, S., Matsui, E., Okino, K., Takenaka, H., Sato K., Kyusho, Y. and Washio, K. Efficient and high-quality overlap welding of car-body aluminum alloy metal sheets with high power Nd:YAG lasers by flexible fiber beam delivery. *Proceedings of*

Laser Advanced Materials Processing, (Ed.) A. Matsunawa and S. Katayama, 1992, pp.517-522.

6. Lawrence, F. V. Jr. and Munse, W. H. Effects of Porosity on the Tensile Properties of 5083 and 6061 Aluminum Alloy Weldments. *Engineering Foundation Welding Research Council Bulletin.* Vol. 181, pp. 1.

7. Ashton, R. F., Wesley, R. P. and Dixon, C. R. The Effect of Porosity on 5086-H116 Aluminum Alloy Welds. *Welding Journal.* March 1975, vol. 54, no. 3, pp. 95-98-s.

8. Sakamoto, H., Shibata, K. and Dausinger, F. Laser Welding of Different Aluminum Alloys. *Proceedings of ICALEO '92 Laser Materials Processing, 25-29 Oct. 1992.* Orlando, Florida, pp. 523-528.

9. Simidzu, H., Yoshin, F., Katayama, S. and Matsunawa, A. *Proceedings of Laser Advanced Materials Processing*, (Ed.) A. Matsunawa and S. Katayama, 1992, pp.511-516.

10. Luciani, P. Y., Charissoux, C. and Calvet, J. N. CO_2 laser auxiliary source couplings: application to welding. *Proceedings of the 3rd International Conference on LASERS in manufacturing, 3-5 June 1986.* Paris, France, pp.117-123.

11. Abedl-Rahman, Mamduh et. al. Formation Energy in Al-Mr Alloy by Positron Ammihilation Lifetime Technique (PALT). *Turk J Phys 26 (2002), 381-389.*

12. Li, L. The advances and characteristics of high-power diode laser material processing. *Optics and Lasers in Engineering*. 2000. vol. 34, pp. 231-253.

13. Heyden, J., K. Nilsson, and C. Magnusson. 1990. *Industrial Laser Handbook.* p.161.

14. Bagger, C., Miyamoto, I., Olsen, F. and Maruo, H. *Proceedings of LAMP1992.* p.553.

15. Chandler, H. Hardness Testing Second Edition. Materials Park, Ohio: ASM International, December 1999.

16. Carslaw, H. S. and Jaeger, J. C. Conduction of Heat in Solids. Oxford: Oxford University Press, 1959.

17. Charschan, Sidney S. Guide to Laser Materials Processing. Orlando: Laser Institute of America, 1993.

CHAPTER 4. CO_2 LASER WELDING OF GALVANIZED STEEL SHEETS USING VENT HOLE APPROACH

A paper submitted to the Journal of Materials Processing Technology

Weichiat Chen, Paul Ackerson and Pal Molian

Abstract

Hot-dip galvanized steel sheets of 0.68 mm (24 gage) thick that contained vent holes at the weld location were welded in the lap joint configuration using a 1.5 kW continuous-wave CO_2 laser in near-Gaussian mode. The vent holes were pre-drilled using a pulsed Nd:YAG laser. This novel "vent hole" approach allowed the zinc vapors to escape through the weld zone without causing expulsion of molten metal and associated defects such as porosity, spatter, and loss of penetration. The quality of the welds was evaluated through optical and scanning electron microscopy and tensile/hardness tests. Results are compared with those obtained in the conventional procedure of a constant joint gap between the sheets.

Introduction

Laser welding constitutes the second largest segment of laser manufacturing applications market with a share of about 40%. It is widely known for its deep penetration (keyhole welding) capability for welding thick metals (> 1 mm), although it can be successfully used in the conduction-mode for thin-sheet metal welding. Laser welding of galvanized mild steels in thickness range of 0.6 - 1.5 mm (0.024 – 0.059 in.) is extensively implemented in the automotive industry for tailored blank welding applications. The zinc

coating on the steel is generally less than 10 μm on each side (an estimated weight of 0.04 – 0.06 kg/m^2); occasionally thicker than 20 μm for added protection [1]. Laser welding is most preferred over mash seam welding for galvanized steels because of the benefits such as high speed, low heat input per unit volume, improved corrosion resistance, fiber optic beam delivery and ease of interface with robots [2].

In comparing the two most widely used welding lasers - CO_2 and Nd:YAG - the CO_2 remains as the workhorse for the industry because it is reliable and most efficient (output efficiency can approach 30%) in addition to offering wider power range and lower operating costs [3]. Most importantly, the CO_2 laser offers a higher welding speed than the Nd:YAG laser. Previous work [4] shows that full penetration welds were obtained in 0.8 mm thick galvanized steel sheets in lap-joint configuration with a relatively slow speed of 2.8 m/min by using a 1.3 kW average power pulsed Nd:YAG laser. In this paper, we are able to show that much faster welding can be obtained in welding 0.68 mm thick galvanized steel sheets with a 1.5 kW CO_2 laser.

A study of CO_2 laser welding of 1.78 mm (0.07 in.) and 0.89 mm (0.035 in.) thick steel sheets in lap-joint configuration shows that the presence of interface has little effect on the shape or dimensions of the fusion zone [5]. However, due to the zinc's relatively low boiling point (906°C, 1663°F) as compared to the melting temperature of steel (1530°C, 2786°F) [6], the zinc coating tends to evaporate during the welding process (see Figure 4.1). Assuming that there is no joint gap in lap configuration, the vaporized zinc is pressurized until it sees the keyhole that permits a larger weld depth [7]. When the keyhole enters the interface, the pressure destabilizes the keyhole and the bubbles of vaporized zinc will attempt to escape through the keyhole. Zinc vapor causes damage to the weld zone and development

of pores in the seam, resulting in poor surface quality, reduced strength, and inferior corrosion resistance [8]. This problem is usually corrected in the industry by introducing a joint gap between the sheets. A theoretical model [9] predicts the gap, g, by equating the volume of zinc vapor generated per second at the interface to the rate of escape of vapor through the gap:

$$g = K\, V\, t_{zn}\, t_p^{-1/2} \qquad (4.1)$$

where K = constant (18.25 $sec.m^{-1/2}$ for CO_2 laser), V = welding speed, t_{zn} = thickness of coating, t_p = sheet thickness. If g/t_p is about 0.25, good quality welds were obtained. If "g" is less than 0.25 t_p, then some blowout in the weld occurs. In practice, the recommended value for the gap is 0.1 mm. This gap size works very well under controlled conditions but maintaining a constant gap is often difficult in production line because the lap joint, for example, may follow a curved surface. Hence, *the industry seeks an alternative to eliminating the gap constraint.*

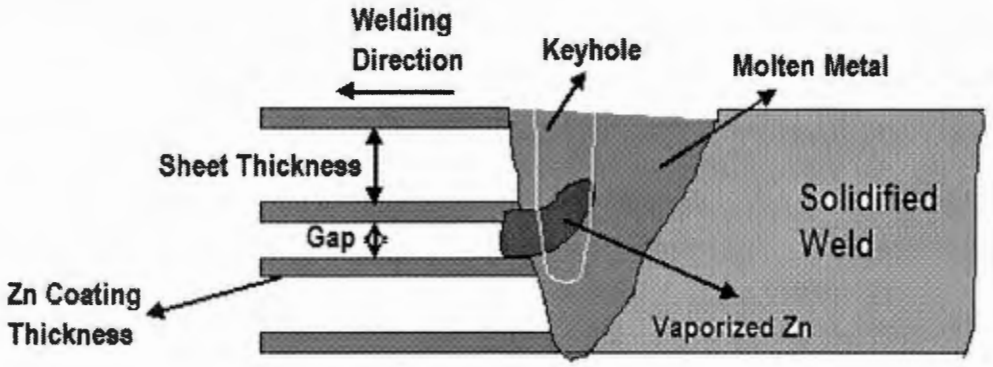

Figure 4.1. Schematic of welding galvanized steel in lap-joint configuration

Studies [1, 9-11] demonstrate that the pressure that inflicts the damage depends on the relation between the sheet thickness and coating thickness. For example, if the coating thickness is less than 7 μm for a 0.8 mm sheet thickness, the pressure effect becomes insignificant. However, if the coating thickness is larger, then explosive vaporization of zinc occurs. Thus, the problem is aggravated by increased coating thickness. Consequently, there is a restriction on the coating weight/thickness at the joint interface.

Another problem in laser welding of galvanized steels is the severe plasma formation due to low boiling point and high vapor pressure of zinc (which is about eight orders of magnitude greater than that of iron). For plasma temperatures of 10,000 K, the electron density of Zn (2.2×10^{18} cm^{-3}) is two orders of magnitude greater than that of Fe (4.1×10^{16} cm^{-3}) suggesting that Zn gives rise to a strongly ionized plasma. The electron density affects the absorption and scattering of incident radiation and prevents the beam propagation through the Zn plasma. The vapor pressure causes the plasma to expand further into the free space affecting absorption of laser energy and plasma fluctuation. This, in turn, not only increases the *spatter* and *porosity* but also reduces the *penetration.* The perturbations taking place during the laser-plasma interactions can cause s*eam discontinuity* and *seam narrowing.*

The central issue in laser welding of galvanized steel is the ability to vent out the zinc vapors or remove the zinc prior to welding. Currently, fairly acceptable laser welds are produced by introducing a small clearance (joint gap) between the sheets in lap welding, usually in the range of 0.1 mm – 0.2 mm (0.004 in. – 0.008 in.), depending on the type of coating, thickness of coating and steel sheet, laser parameters and welding speed [6].

However, the techniques for better venting the zinc vapor are highly sought after. Consequently, a number of alternative ideas are proposed as shown in Table 4.1.

Table 4.1. Potential alternatives to providing joint gap in laser welding of galvanized steels.

Method	**Drawbacks**
Remove the galvanized layer at the joint interface prior to welding	Expensive in production environment
Pre-drill holes in the steel sheet facilitating an escape route for zinc vapors	Additional processing
Fill the joint gap with porous, powdered metal that will provide room for zinc vapors to pass through.	Difficult to implement in production environment.
Use pulsed lasers that have high energy per pulse and short pulse duration to minimize vaporization	Keyhole may not occur
Dual-beam hybrid or shaped beam techniques that will give rise to pre-heating effects to eliminate zinc	Complex equipment
Addition of a small amount of oxygen (2 to 5%) to argon to allow the zinc to react with oxygen and reduce its explosive effect	Flow rate conditions must be optimized to dissipate the plasma; oxide porosity

In this work, we have attempted a novel approach of drilling vent holes on the bottom sheets prior to welding; these vent holes work as pressure-relieving points along the weld

zone. The vent holes allow the zinc vapor to escape and the liquid metal to flow into the vent holes freely, thus creating rivet-shaped welds along the weld seam. In this paper, we report a comparison of weld quality of CO_2 laser welding of galvanized steel using "no gap", conventional "joint gap", and "vent hole" approaches.

Experimental Details

Hot-dip galvanized steel sheets of 24-gage thickness (38.1 x 38.1 x 0.68 mm) with a coating thickness of 7 μm were procured and surface cleaned with methanol. The vent holes were drilled using a pulsed Nd:YAG laser on the bottom sheets with an arbitrary spacing of 10 mm (Figure 4.2). The laser parameters (average power: 400 W, pulse width: 1 msec, pulse frequency = 50 Hz, assist gas: air) were controlled to produce holes with a nominal diameter of arbitrary 700 μm. Burr formation occurred at the bottom of holes and provided further ability to act as a joint gap in conjunction with the vent holes.

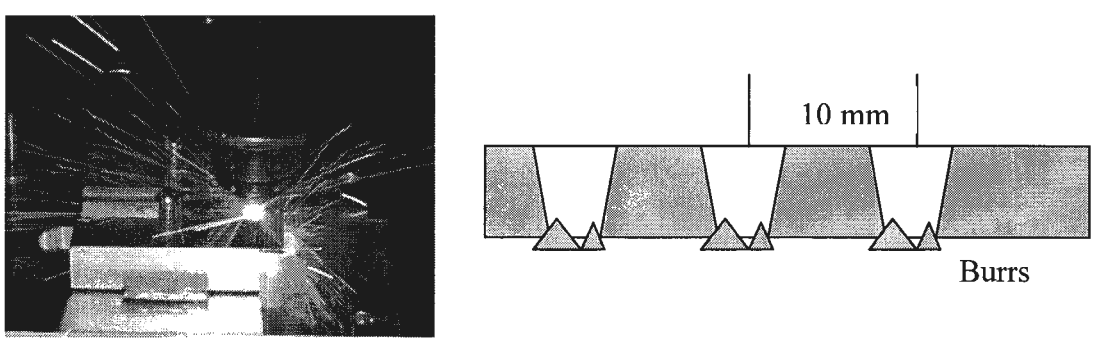

(a) **(b)**

Figure 4.2. (a) Drilling of vent holes in galvanized steel sheets using a 400 W pulsed Nd:YAG laser, (b) pattern of holes produced.

Sheets were then held in a lap-joint configuration using a clamping device to provide support, keep the sheets in contact, and for the quick release of specimens (Figure 4.3a). A feeler gauge was used to vary the joint gap by raising one sample above the other and ensuring an even height across the surfaces. A 1.5 kW continuous wave CO_2 laser in near TEM_{00} mode with a spot size of 0.2 mm was used to weld the sheets (Figure 4.3b). Since a 2 kW CO_2 laser is able to achieve a weld depth of 3 mm for steel at welding speed of 1 m/min [9], much faster welding than 1 m/min were employed. Gas shielding plays an important role in laser welding. In this case, argon was used as the assist gas during the welding process not only to prevent the effects of moisture and contamination that otherwise triggers porosity and cracking [10, 11], but also to protect the laser beam from power loss during its transmission from the lens to the sheets [12]. A blue/white plasma plume consisting of ionized and neutral particles was generated during welding as seen in Figure 4.3b.

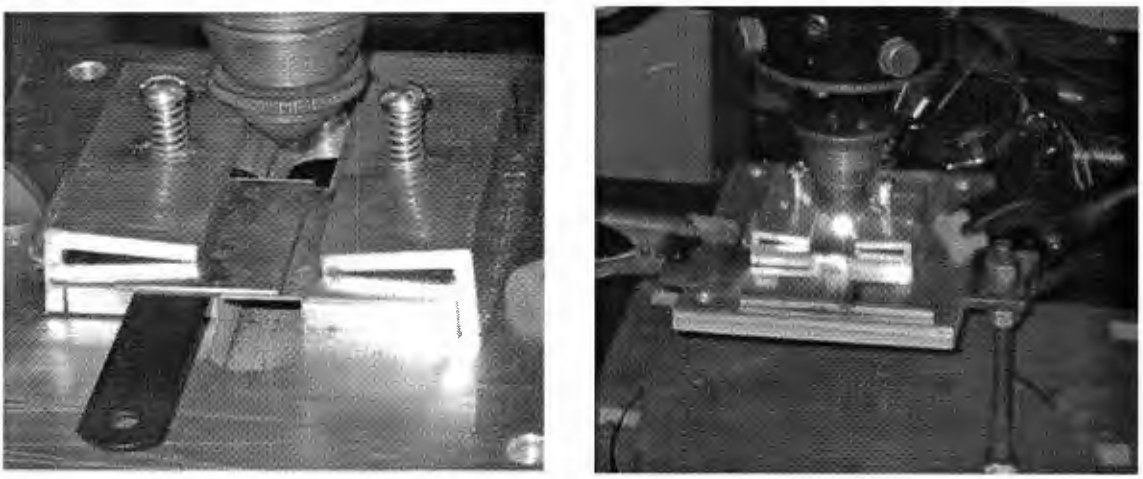

Figure 4.3. (a) experimental setup for CO_2 laser welding; and (b) actual CO_2 laser welding of galvanized steel.

Three types of experiments were carried out: 1) "no gap" approach, where the sheets were secured by a clamp directly above the slot to ensure that the clearance between the two sheets is as close to zero as possible. Throughout the experiments, the clamp was mounted on a linear motion table that is numerically controlled by a computer; 2) "joint gap" approach where a filler gauge was used to provide a clearance of 0.127 mm (0.005 in.); and 3) "vent hole" approach where the top sheet was placed above the pre-drilled bottom sheet, and secured under the clamps. The 5 mW He-Ne laser beam, which has a visible red color and a safe power level [12], was used to align the CO_2 laser beam to the marked seam (on the top sheet, directly above the drilled vent holes). A few trail runs were conducted to ensure that the He-Ne beam illuminates the marked seam at all times. The welding process was carried out using the CO_2 laser and shielding gas. The welding speed was varied from 5 m/min to 10 m/min, while all other variables were kept constant.

The integrity of the welds was evaluated using optical microscope (grain structure), scanning electron microscope (weld flaws) and tensile/hardness tests (strength). Welded sheets were mounted in bakelite and copper powders for metallographic examination. Mounting the samples in this fashion facilitates handling the thin samples during grinding and polishing prior to microscopic examination [13]. The samples were then etched in natal (10% nitric acid and 90% methanol) [14] for optical and SEM imaging. Welds obtained with varying welding speeds were evaluated for strength under the standard tensile test. Vickers micro hardness, and Rockwell A, and Rockwell C macro hardness tests were also used to measure the hardness of welds.

Results and Discussion

Figure 4.4a shows an optical micrograph of a representative transverse section of "no gap" approach weld where the vaporization of zinc created a pressure build-up between the sheets, causing turbulence in the molten puddle and resulting voids in the weld as well as a large gap between the top and bottom sheets. A backscattered electron imaging of the weld (Figure 4.4b) shows the evidence of porosity in the weld. These results infer that excessive zinc vapor that was trapped in the solidified weld affected the flow of molten metal and formed gas pockets.

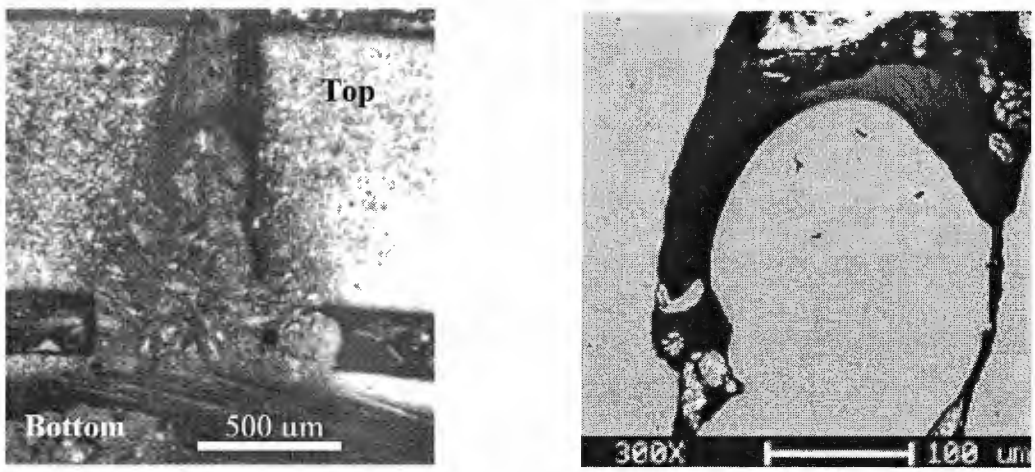

(a) **(b)**

Figure 4.4. Transverse section of weld produced by "no gap" approach; the weld profile shows incomplete penetration, void, gas porosity and a gap between the sheets.

Figures 4.5a and b depict a typical longitudinal weld, representative of the "joint gap" and "vent hole" approaches. Visual examination of many of these welds indicated that good welds were obtained in the speed range of 6 to 8 m/min. Figure 4.5c shows the "best

possible" transverse section of the keyhole laser weld in the lap-joint configuration achieved through the "joint gap" approach.

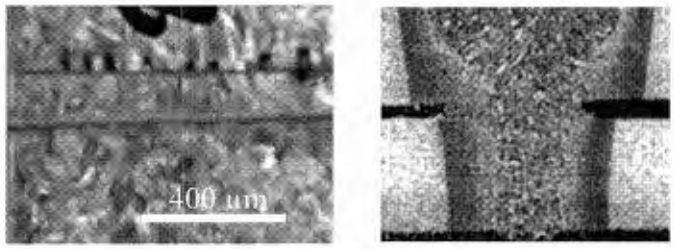

(a) (b)

Figure 4.5. Optical micrographs of laser welded galvanized steel: (a) longitudinal section of weld, (b) transverse section of weld in lap-joints using "joint gap" approach.

Weld flaws were also present in the "joint gap" approach. Figures 4.6a to c are the optical and scanning electron images of the transverse sections of weld profiles with a "joint gap". Figure 4.6a shows large voids at the interface between two sheets. The zinc vapor pressure build-up during the welding process further enlarged the original gap between the top and bottom sheets. The extreme pressure build-up also induced severe disturbance to metal flow and generated undercutting as well as cracking within the weld. It is seen that that cracks have formed along the edges where the zinc coating was present. This is confirmed by the energy dispersive spectrum of the weld near the crack (Figure 4.6c). Methods for eliminating the cracking in laser welding include bevel-cutting the edges and/or removing the zinc coating from the surfaces [15, 16]. There were no signs of fine porosity within the weld, indicating that the clearance intentionally placed between the top and bottom sheets was adequate in venting the zinc vapor during welding.

Figure 4.7 shows macro-views of longitudinal laser welds produced in the vent hole approach. Analysis revealed that the welds were dense free of porosity and voids. There was no effect of excessive zinc vapor and pressure build-up between the sheets on the quality of the joint. The zinc was uniformly distributed throughout the weld zone. Figure 4.8 shows the optical micrographs of transverse sections of welds that did not indicate any sign of cracking. Figure 4.9 illustrates the formation of rivets at the locations of pre-drilled holes in the longitudinal sections of the bottom sheets where the molten metal is being directed into the vent holes during welding process.

Tensile tests were conducted to analyze the integrity of the joints produced by the welding approaches. For each case, two samples were pulled apart and the average values were plotted. Figure 4.10 shows that the tensile load decreases with increasing welding speed due to the decreasing weld penetration. Welds produced in "vent holes" configuration have higher tensile strength than those produced in "joint gap" configuration. It is hypothesized that the molten metal has adequate time to channel into the vent holes, forming rivet-shaped welds, thus giving rise to higher tensile strengths. However, at very high welding speed, the tensile load-carrying capacity for the "vent hole" welds is lower than those of "joint gap" welds partly because the liquid metal was not able to penetrate into the gap by gravitational force alone. In addition, the undercut in "joint gap" weld is minimized at higher welding speeds as a result of faster cooling rate of the weld pool.

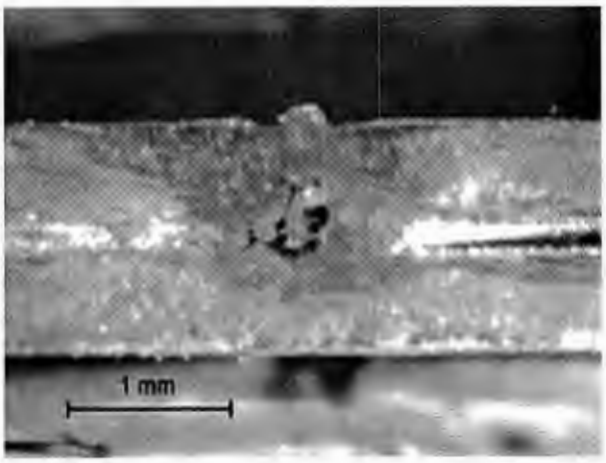

(a)

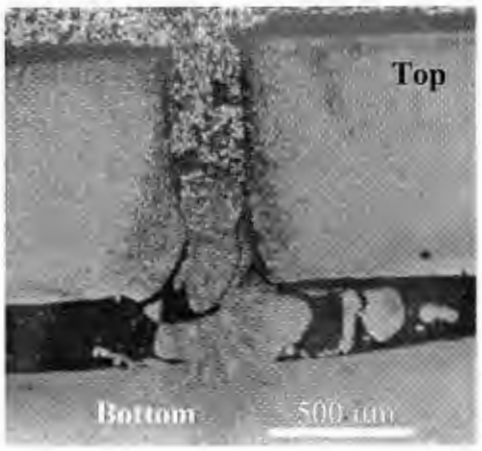

(b)

(c)

Figure 4.6. Weld flaws associated with "joint gap" approach (a) Optical micrograph showing large voids at the interface, b) Optical micrograph showing the undercuts and cracks in the fusion zone; (c) Energy dispersive spectrum showing the presence of only zinc at the crack location.

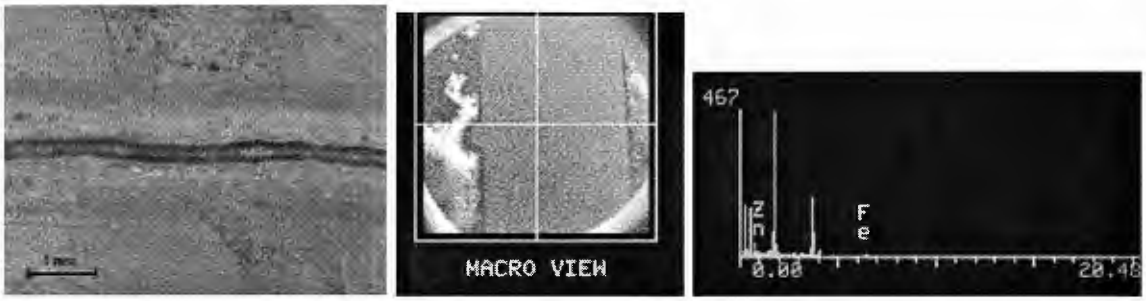

(a) (b) (c)

Figure 4.7. (a, b) Longitudinal section of lap-welded sheets using the "vent hole" approach. Note the bead at the end of the weld in b. (c) Energy-dispersive X-ray spectrum of the weld zone.

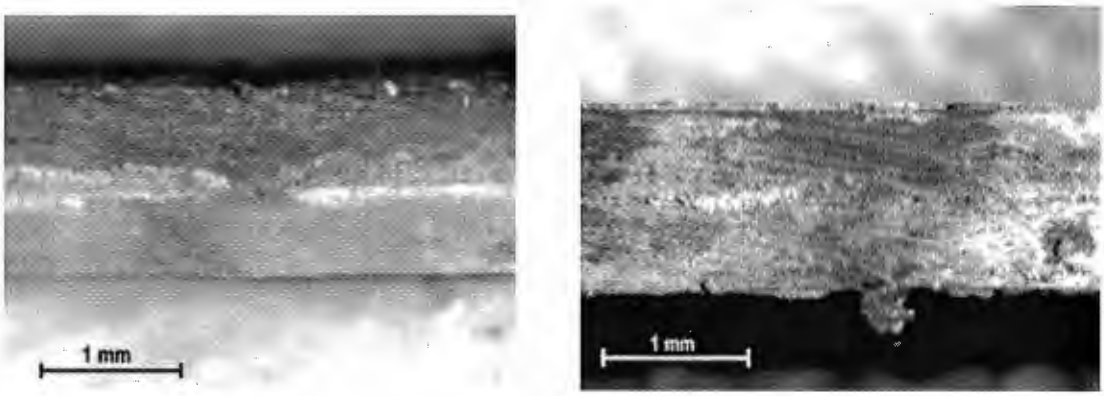

(a) (b)

Figure 4.8. (a, b) Transverse sections of lap-welded sheets using the "vent hole" approach show no evidence of cracking in both the weld and bead.

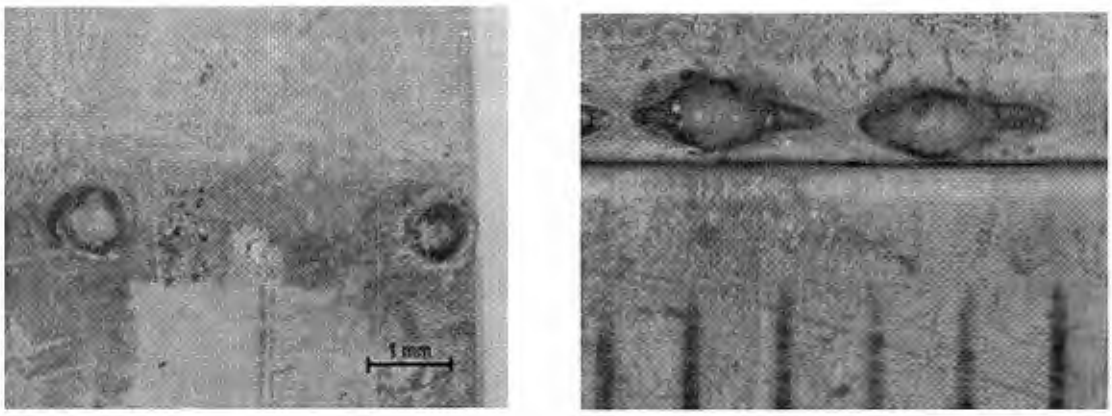

(a) (b)

Figure 4.9. Rivet-shaped welds produced under welding speed (a) 7.62 m/min (300 ipm), (b) 5.08 m/min (200 ipm). Note that line spacing in (b) is equal to 1 mm.

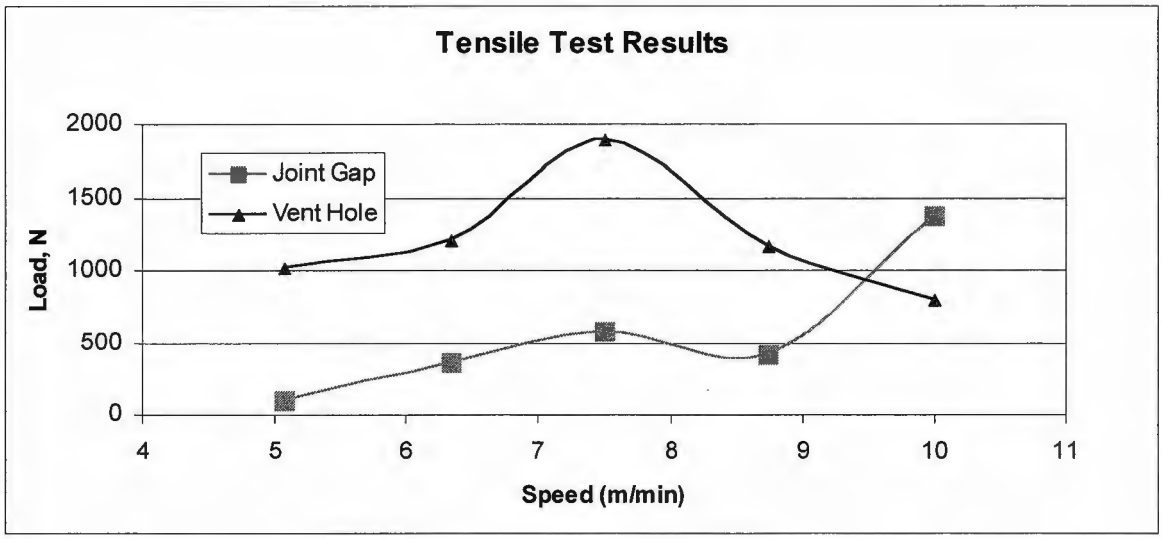

Figure 4.10. Tensile test results plotted as welding speed as a function of tensile load

Figure 4.11 is a histogram chart of hardness test results of the welds produced under "no gap", conventional "joint gap", and "vent holes" approaches. Hardness test results were plotted in three scales: Vickers, Rockwell A, and Rockwell C scales for easy conversion. The

overall hardness of the welds is close to three times the hardness of the base steel, which has a Vickers Hardness Number (VHN) of 138. The increased hardness is attributed to the formation of finer grain structure within the weld than that of the base metal. A steep temperature gradient between the high temperature melt and the base metal causes a high cooling rate [17]. Fine grain structure is produced as a result of high cooling rate of the melt. The small increase in hardness in "joint gap" and "vent hole" approaches compared to the "no gap" joints is due to the absence of gas porosity.

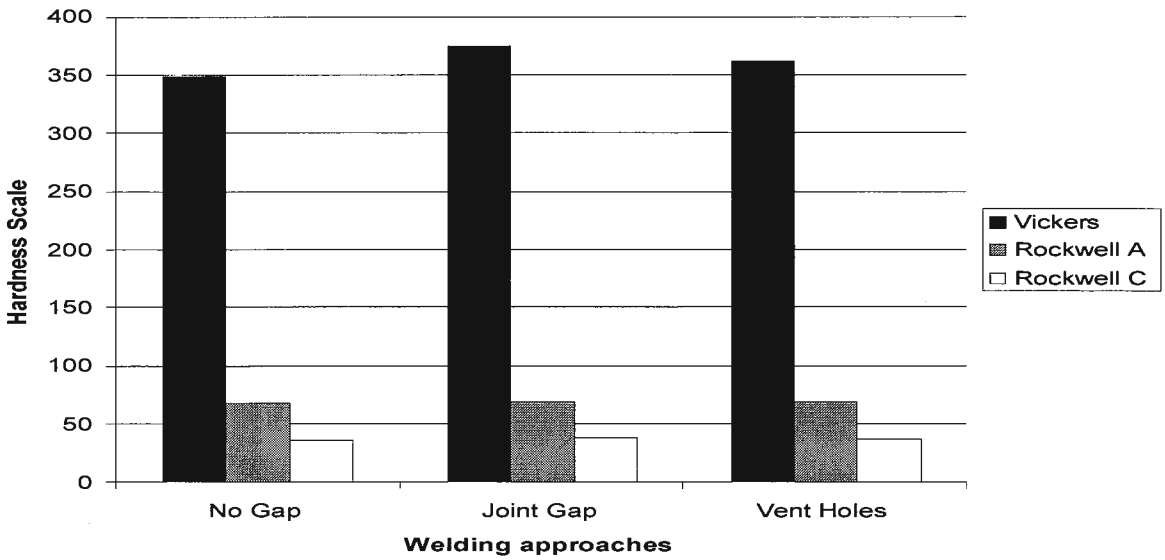

Figure 4.11. Hardness test results

The results for the CO_2 laser welding using a novel approach of vent holes have shown that better welds are achieved when compared with the existing "joint gap" method. The advantage of vent hole approach is it's industrially viability with minimal setup time and cost effectiveness. An issue of consideration is the size of vent hole in relation to the weld

width. It was noted that the weld width was larger than the hole diameter by about three times. This raises the question of whether it is proper to have a vent hole with a diameter larger than that of the weld width. Although larger vent holes justify the elimination of deleterious effects of zinc and possibly increased strength, vent holes smaller than the weld width provide the mechanism of riveting and increased adhesion. The burrs that were left on the bottom sheet also assisted in venting of zinc vapor prior to the formation of weld pool. This explains the successful dispersion of zinc in "vent hole" weld. It also made the weld concavity to minimum. The positioning of the holes is a critical factor. In the experiments, the holes were placed directly along the weld line with a minimum spacing calculated by the following finite-element analysis.

The weld configuration is depicted in Figure 4.12. The half-width of the weld is taken as 0.1 mm based upon experimental data. This is used as the reference edge. The contact edge is assumed to be at 1530°C (vaporization temperature of steel), and the opposite edge is assumed to be at 25°C (room temperature). The position of the edge of the vent hole is decided on the basis that the temperature must be 906°C (vaporization temperature of zinc) when the beam crosses it. FEM results plotted in Figure 4.13 suggest that the vent holes should be spaced 0.14 mm apart to allow the zinc vapors to escape through prior to the formation of weld pool.

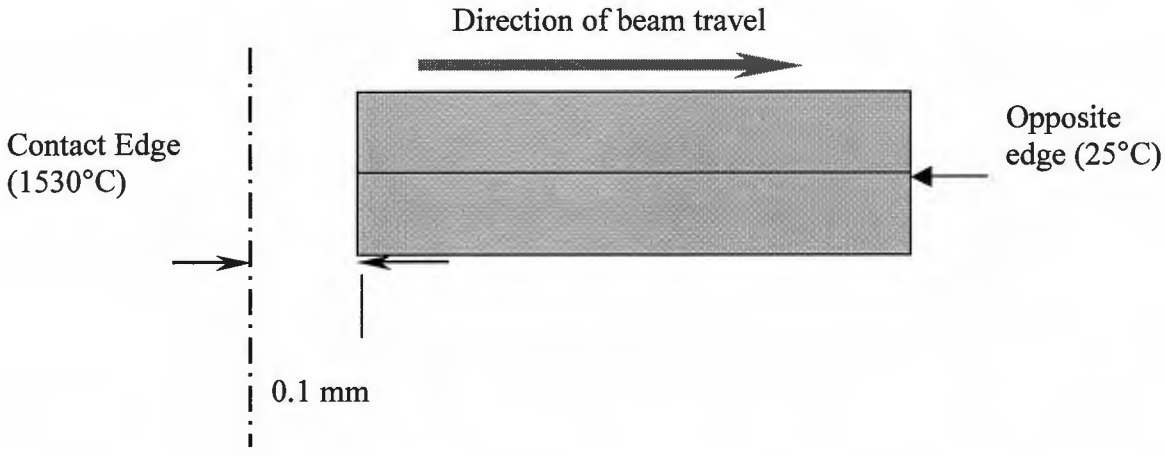

Figure 4.12. Geometry for identifying hole spacing in vent hole method

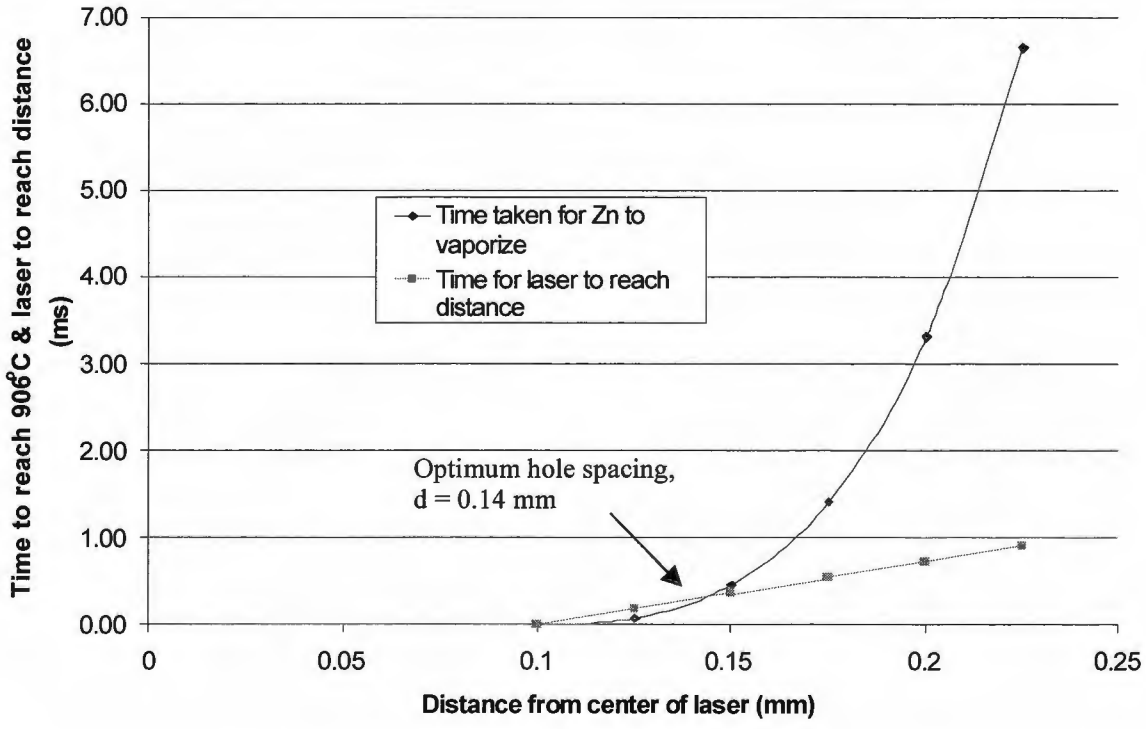

Figure 4.13. FEM analysis results of heat transmission in laser heating

Conclusions

The current problem in laser welding of galvanized steel in the lap joint configuration is the vaporization of the zinc during welding process. While a clearance between the sheets overcame this problem, this "joint gap" method is becoming difficult to implement in the industry. In this paper, we have presented an alternative approach of using vent holes that allowed formation of much stronger welds through riveting mechanism and offered adequate venting of zinc. This approach reduced the most common defects associated with galvanized steel welding. Results also inferred that there is a relationship between the weld width and spacing of vent holes. Finite element analysis revealed that the optimum spacing between holes is 0.14 mm so that zinc will be removed prior to melting of steel.

Acknowledgements

The authors would like to thank Professor J. N. Gray (Center for Non-Destructive Evaluation, Iowa State University), Professor Scott Chumbley (Ames Laboratory), and Mr. John Meyers (Ames Laboratory), for providing their help and expertise in NDE and microscopy.

References

1. Ayres, K. R. and P. A. Hilton. "CO_2 laser butt welding of coated steels for the automotive industry." *Welding and Metal Fabrication.* January 1994, pp. 10-12.
2. Pizzi, P. "Lasers in automotive production." Laser Welding, Cutting and Surface Treatment. Cambridge, England: The Welding Institute. 1984, p. 40.

3. Duley, W. W. Laser Welding. New York: John Wiley & Sons, Inc., 1999.

4. Norris, I., Peters, C., and Wileman, P. "Welding with a 3kW Nd:YAG Laser." *ICALEO '92 Laser Materials Processing.* October 1992, session 1, pp. 53-62.

5. Baardsen, E. L., Schmatz, D. J., and Bisaro, R. E. "High Speed Welding of Sheet Steel with a CO_2 laser." *Welding Journal.* Apr. 1973, vol 52, no. 4, pp. 227-229.

6. Xie, J. and P. Denney. "Galvanized Steel Joined with Lasers." *Welding Journal.* June 2001, vol. 80, no. 6, pp. 59-61.

7. Duley, W.W. CO_2 Lasers Effects and Applications. New York: Academic Press, Inc., 1976.

8. Seyffarth, P. and I. V. Krivtsun. Laser-Arc Processes and their Applications in Welding and Material Treatment. Lodon, UK: Taylor & Francis Inc., 2002, pp. 166.

9. Akhter, R., W. Steen, and D. Cruciani, Proceedings of 5th International Conference on *Lasers in Manufacturing, LIM 5,* 13-14, Sep.1988, Stuttgart, Germany, p.195

10. Heyden, J., K. Nilsson, and C. Magnusson,1990, Industrial Laser Handbook, p.161

11. Bagger, C., I. Miyamoto,F.Olsen, and H. Maruo, *Proceedings of LAMP1992*, p.553

12. Dawes, C. J. "An introduction to CO_2 laser welding low carbon steel up to 4mm thick." *Developments And Innovations for Improved Welding Production: 1st International Conference.* Cambridge, England: The Welding Institute. 1984, pp. 43-1 - 43-10.

13. "Checking the Quality of a Laser Weld." *Welding Journal.* July 1979, 59, 7, pp. 53-54.

14. Prevey, P.S., "Residual Stress Distributions Produced by Strain Gage Surface Preparation." *Proc ., 1986 SEM Conference on Experimental Mechanics* (1986).

15. Gregory, E. N., "Welding zinc-coated steels." Welding Coated Steels. Cambridge, England: The Welding Institute. 1978, pp. 5-12.

16. Bland, J. Welding Zinc-Coated Steel. Miami. Florida: American Welding Society, Inc., 1972, p. 94.

17. Moon, D. W. and E. A. Metzbower. "Laser Beam Welding of Aluminum Alloy 5456." *Welding Journal.* Feb 1983, vol 62, no. 2, pp. 53s-58s

CHAPTER 5. GENERAL CONCLUSIONS

Dual-beam laser welding proves to be a feasible and superior method of joining aluminum alloys that provides far better weld quality in terms of deeper weld penetrations and higher tensile strengths than that of single-beam laser welding. By adding another flexible and fairly inexpensive diode laser to an existing welding laser, better welding results are obtained whether the auxiliary laser was used as a pre-heating, same position heating, or afterheating source. More laser energy was able to be coupled to the material due to lower reflectivity of the nature of the incident beam of the short wavelength diode laser.

A good portion of the industry is using the "joint gap" method to assist expulsion of zinc vapors during galvanized steel welding process. This method is particularly difficult to implement while a clearance between the sheets overcame this problem. The alternate "vent hole" approach offers the simplicity of eradicating the need of placing a feeler gauge between the galvanized sheets to provide a constant gap in the "joint gap" method. In addition to adequate venting of zinc vapors, this "vent hole" approach allowed formation of much stronger welds through riveting mechanism between the sheets.

APPENDIX: THERMAL PROPERTIES AND SAMPLE CALCULATIONS

Aluminum alloy 5052 thermal properties

K	1.38	w/cm-°C	thermal conductivity
ρ	2.68E+03	kg/m3	density
Cp	963	J/kg-°C	specific heat
Tm	649	°C	melting temperature
R	0.76		reflectivity
k	0.9	cm2/s	thermal diffusivity
Lf	3.96E+05	J/kg	latent heat of fusion

Dual-beam welding surface temperature profile (welding speed = 0.9 m/min)

Time, s	Surface Temp, °C
0.010	189.6
0.016	239.9
0.020	158.7
0.030	109.5
0.040	89.6
0.050	77.8
0.060	69.8
0.067	1339.6
0.080	456.4
0.090	427.4
0.100	403.3
0.110	382.9
0.120	365.3
0.130	349.9
0.140	336.3
0.150	324.2
0.160	313.3
0.170	303.5
0.180	294.5
0.190	286.2
0.200	278.7

Sample calculations

Diode laser (preheating beam)

Beam spot diameter, 2a = 0.025 cm

Spot area, $A = \frac{\pi}{4}(2a)^2 = 0.0005cm^2$

Incident power density, $I_o = \frac{P}{A} = \frac{5W}{0.0005cm^2} = 10186\frac{W}{cm^2}$

Average power density absorbed, $I = I_o(1-R) = 10186\frac{W}{cm^2}(1-0.76) = 2445\frac{W}{cm^2}$

Welding speed, $v = 0.3m/\min = 5mm/s$

Time, $t_p = \frac{2a}{v} = \frac{0.25mm}{5\,mm/s} = 0.05s$

Peak surface temperature in pre-heating

$$T(0,t) = \frac{2I}{K}\sqrt{\frac{kt}{\pi}}$$

$$T(0,0.05s) = \frac{2*2445\frac{W}{cm^2}}{1.38\frac{W}{cm-^oC}}\left[\sqrt{\frac{0.9\frac{cm^2}{s}*0.05s}{\pi}}\right] = 424^oC$$

Time required to travel 1 mm at welding speed of 0.3 m/min

$$t = \frac{1mm}{0.3\frac{m}{\min}\left[\frac{1000mm}{1m}\right]\left[\frac{1\min}{60s}\right]} = 0.2s$$

Surface temperature at $t = 0.2s, t_p = 0.05s$

$$T(0,t) = \frac{2I}{K}\sqrt{\frac{k}{\pi}}\left[\sqrt{t} - \sqrt{t - t_p}\right]$$

$$T(0,0.2s) = \frac{2 * 2445 \frac{W}{cm^2}}{1.38 \frac{W}{cm - {}^oC}}\left[\sqrt{\frac{0.9 \frac{cm^2}{s}}{\pi}}\right]\left[\sqrt{0.2s} - \sqrt{0.2s - 0.05s}\right] = 114^oC$$

Nd:YAG laser (welding beam)

Wavelength	1064 nm
Average output power	2 W
Transverse Mode	TEM_{00}
Beam Diameter, nominal at $1/e^2$ power point	1.2 mm
Focal length	108 mm

Beam mode parameter $M^2 \approx 1$

Beam spot diameter, $2a = \frac{4M^2\lambda f}{\pi D}$

$$= \frac{4(1)(1064nm)(108mm)}{\pi(1.2mm)}\left[\frac{1mm}{1 \times 10^6 nm}\right]$$

$$= 0.061mm$$

Spot area, $A = \frac{\pi}{4}(2a)^2 = 2.922 \times 10^{-5} cm^2$

Incident power density, $I_o = \frac{P}{A} = \frac{2W}{2.922 \times 10^{-5} cm^2} = 68435 \frac{W}{cm^2}$

Average power density absorbed, $I = I_o(1-R) = 68435\frac{W}{cm^2}(1-0.76) = 16424.5\frac{W}{cm^2}$

Welding speed, $v = 0.3m/\min = 5mm/s$

Time, $t_p = \frac{2a}{v} = \frac{0.061mm}{5\,mm/s} = 0.012s$

Peak surface temperature in welding

$$T(0,t) = \frac{2I}{K}\sqrt{\frac{kt}{\pi}}$$

$$T(0,0.012s) = \frac{2*16424\frac{W}{cm^2}}{1.38\frac{W}{cm-^\circ C}}\left[\sqrt{\frac{0.9\frac{cm^2}{s}*0.012s}{\pi}}\right] = 1274^\circ C$$